


9-1-1978

Hydrolytic and Photochemical Degradation of Organophosphorus Pesticides

James F. Hinton

University of Arkansas, Fayetteville

Follow this and additional works at: <https://scholarworks.uark.edu/awrctr>

 Part of the [Fresh Water Studies Commons](#), and the [Water Resource Management Commons](#)

Recommended Citation

Hinton, James F. 1978. Hydrolytic and Photochemical Degradation of Organophosphorus Pesticides. Arkansas Water Resources Center, Fayetteville, AR. PUB063. 74

This Technical Report is brought to you for free and open access by the Arkansas Water Resources Center at ScholarWorks@UARK. It has been accepted for inclusion in Technical Reports by an authorized administrator of ScholarWorks@UARK. For more information, please contact scholar@uark.edu, cmiddle@uark.edu.

Hydrolytic and Photochemical Degradation of Organophosphorus Pesticides

Principal Investigator:

James F. Hinton

Department of Chemistry



Arkansas Water Resources Research Center

University of Arkansas

Fayetteville, Arkansas

Publication No. 63

1978

ARKANSAS WATER RESOURCES RESEARCH CENTER

OWRT Project No. A-030-ARK

Project Title: Hydrolytic and
Photochemical Degradation of
Organophosphorus Pesticides

Matching Grant Agreement No. 14-34-0001-6004
FCST Research Category, V-B

Project Began - June 1974

Scheduled Completion - September 1978

Name and Location of Institution Where Project

University of Arkansas, Fayetteville, Arkansas

Principal Investigators

James F. Hinton

Degree

Ph.D.

Discipline

Physical Chemistry

Postdoctoral

K.H. Ladner

Ph.D.

Physical Chemistry

Student Assistants

Richard W. Briggs

B.S.

Chemistry

ACKNOWLEDGEMENTS

The work upon this publication was supported with funds provided by the Office of Water Research and Technology, U. S. Department of the Interior, through the Water Resources Research Center of the University of Arkansas under grant A-041-ARK as authorized under Water Resource Research Act of 1964, P.L. 88-379 as amended by P.L. 89-404 and P.L. 92-175.

TABLE OF CONTENTS

	<u>Page</u>
A. General Introduction	1
B. Experimental	7
1. Chemicals	7
2. Sample Preparation.	8
3. Acquisition of Spectra.	10
C. Results and Discussion	12
1. Ethyl Parathion	12
2. Methyl Parathion.	17
3. Supracide	17
4. Summary	39
D. Future Research.	52
E. References	54
F. Appendix	57

LIST OF TABLES

<u>Table</u>	<u>Page</u>
1 Structures and Nomenclature for Some Organophosphorus Pesticides	9
2 ³¹ P Chemical Shifts of Some Phosphorus Compounds	13
3 Relative ³¹ P Peak Areas of Ethyl Parathion and Its Degradation Products at 60 ^o c	24
4 Relative ³¹ P Peak Areas of Ethyl Parathion and Its Degradation Products at 70 ^o c	25
5 Relative ³¹ P Peak Areas of Ethyl Parathion and Its Degradation Products at 90 ^o c	
6 Relative ³¹ P Peak Areas of Methyl Parathion and Its Degradation Products at 60 ^o c	34
7 Relative ³¹ P Peak Areas of Methyl Parathion and Its Degradation Products at 70 ^o c	35
8 Relative ³¹ P Peak Areas of Methyl Parathion and Its Degradation Products at 90 ^o c	36
9 Relative ³¹ P Peak Areas of Supracide and Its Degradation Products at 60 ^o c	44
10 Relative ³¹ P Peak Areas of Supracide and Its Degradation Products at 70 ^o c	45
11 Relative ³¹ P Peak Areas of Supracide and Its Degradation Products at 90 ^o c	46
12 Rate Constants and Half-Lives of the Pesticides as a Function of Temperature.	48
13 Thermodynamic Data From Arrhenius Plots of Kinetic Data.	48
14 Effective Relaxation Reagents for ³¹ P NMP Observation of Organophosphorus Compounds	52

LIST OF FIGURES

<u>Figure</u>	<u>Page</u>
1 The Degradation of Ethyl Parathion as Monitored by ^{31}P NMR at 36.43 MHz	15
2 Time Course of the Degradation of Ethyl Parathion at +62.15 ppm and the Formation and Reaction of the Hydrolysis Product $\text{PS}(\text{OH})(\text{OC}_2\text{H}_5)_2$ at +64.0 ppm	18
3 Time Course of the Degradation of Ethyl Parathion at +62.15 ppm and the Buildup and Decay of Products at +64.0 ppm, +53.05 ppm, and +0.8 to +1.9 ppm at 70°C	20
4 The Decomposition of Ethyl Parathion at +62.15 ppm and the Formation and Decay of Products at +64.0 ppm, +53.05 ppm and +0.8 to +1.9 ppm at 90°C	22
5 The Degradation of Methyl Parathion as Monitored by ^{31}P NMR at 36.43 MHz	28
6 Plot of Relative ^{31}P Peak Areas vs. Time for Methyl Parathion at +65.75 ppm, and for Degradation Products at +55.4 ppm, +17.0 ppm, and +1.5 ppm.	30
7 Relative ^{31}P Peak Areas as Functions of Time for Methyl Parathion at +65.75 ppm, and for Degradation Products at +55.4 ppm, +17.0 ppm and +1.5 ppm.	32
8 The Degradation of Supracide as Monitored by ^{31}P NMR at 36.43 MHz.	37
9 Time Dependence of the ^{31}P Peak Areas During the Degradation of Supracide at +95.20 ppm to Products at +65.2 ppm, +34.2 ppm, and +1.85 ppm	40
10 Time Dependence of the ^{31}P Peak Areas During the Degradation of Supracide at +95.20 ppm to Products at +65.2 ppm, +34.2 ppm, and +1.85 ppm	42
11 Arrhenius Plot for Degradation of Ethyl Parathion, Methyl Parathion, and Supracide.	49

A. General Introduction

To keep pace with demands for increasing food supplies to satisfy the expanding world population, modern agriculture has utilized the latest scientific and technological knowledge available. Increases in crop production through the use of growth regulators, fertilizers, herbicides, and insecticides have been little short of phenomenal, and drugs, feed additives, and higher-quality grain and forage have dramatically increased livestock production. But, as is usually the case, this progress has been accompanied by problems, one of the more serious being contamination of our environment by chemicals. Only in recent years have the full effects of these pollutants on the ecological balance of nature begun to be understood in all their intricacies and implications.

While probably not as guilty of air and water pollution as are urban industries, rural agriculture is doubtless one of the major contributors to pollution of our natural water systems, in large part because of the widespread use of herbicides and pesticides. Granting that use of these chemicals should be continued, of necessity, to maintain and increase present levels of food production, the problem remains of how to accomplish this with minimum adverse environmental effects. The ultimate goal - an increasingly difficult one in view of today's increasingly sensitive and sophisticated instrumentation - is to do so with no detectable destruction of the ecological balance.

With regard to environmental contamination by pesticides and herbicides, there are several important questions to be considered:

- (1) What are the biological effects of these chemicals? Are they harmful to desirable flora or fauna, and if so, in what way, and in

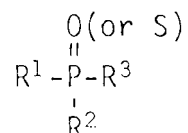
what quantities? (2) What are the stabilities of these compounds? How quickly do they degrade? This is a critical consideration for potentially harmful substances. (3) What is (are) the mode(s) of degradation? How do sunlight, temperature, and additional chemicals and substances native to the environment affect the rates and pathways of decomposition? (4) How is the pesticide transported in the environment? Will factors (1)-(3) vary with geographical region? Will the pesticide be transported through the wildlife food chain and threaten the well-being or even existence of some animal species?

This research project was begun with the goal of providing both qualitative and quantitative answers to queries (2) and (3) of the previous paragraph, for a series of organophosphorus pesticides. These compounds are of importance because of their effectiveness and relatively rapid breakdown; the environmental persistence of other equally effective types of chemicals has in many instances caused them to be banned from private and commercial use as pesticides. Identification of the individual degradation products and determination of the rates of reaction for the various pathways under different conditions is necessary if the fate of these pesticides in our rivers, streams, and lakes is to be completely understood.

Since the initial discovery of the physiological effects of organophosphorus molecules in 1932, much synthetic and toxicological research has been performed on these compounds. Many of the compounds first developed were extremely toxic to mammals as well as to insect pests; derivatives were later synthesized which had a much higher selectivity. The use of organophosphorus pesticides is now widespread:

over 140 phosphorus compounds have been employed as pesticides, with the current annual production now more than 60,000 tons in the United States alone (1).

All biologically active organophosphorus compounds have an acid anhydride linkage, with the general formula



where R^1 and R^2 can be alkyl, alkoxy, or amino groups, and R^3 can be any acid residue (1). The pesticidal activity of these species is due to inhibition of the cholinesterase enzymes, which hydrolyze acetylcholine to choline and acetate. Acetylcholine is one of several important neurotransmitters which transport nerve impulses across the synaptic gap from neuron to neuron. The synaptic gap is 200-300 Å in neural synapses and 500-600 Å in neuromuscular junctions.

Normal cells possess a concentration gradient of K^+ and Na^+ ions, in which the intracellular concentration of K^+ is larger than the extracellular concentration, and vice versa for Na^+ . In nerve cells, this produces a Nernstian potential, the resting potential, of the order of 60-70 mV across the membrane, with the inside being negative with respect to the outside. The resting potential is approximately the equilibrium potential of K^+ . Upon excitation, the membrane's permeability to Na^+ increases about 500-fold, Na^+ ions pass rapidly into the cell interior, and the membrane potential changes quickly from the resting potential of about -70 mV to about +30 mV, approximately the Na^+ equilibrium potential. As the membrane depolarizes during formation of the action potential voltage spike, Na^+

conductivity decreases and K^+ conductivity increases, thus reestablishing the resting potential. The nerve impulse, in the electrical form of the action potential, propagates along the axon until it reaches the nerve ending, where acetylcholine is stored in synaptic vesicles. These normally burst in a spontaneous, intermittent fashion, releasing small amounts of acetylcholine and producing small, 1-2 mV depolarizing potentials. However, the arrival of the action potential at the synapse stimulates the vesicle disruptions and induces a rapid increase of two to three orders of magnitude in the concentration of free acetylcholine, which migrates across the synaptic gap to bind with receptor sites on the postsynaptic membrane of another neuron (or a muscle cell). This binding changes the permeability of the postsynaptic membrane, increases cation conductance, and produces the 10-20 mV end-plate, or postsynaptic, excitation potential, which drastically alters the membrane's Na^+ permeability and triggers the next action potential.

In normal neural operation, the acetylcholine in the synaptic gap and near the receptors of the postsynaptic membrane is hydrolyzed by acetylcholinesterase after the action potential is generated, returning the membrane to its normal polarized resting state in preparation for the arrival of the next burst of chemical nerve impulse carriers. If the enzyme is inhibited, the acetylcholine remains in the synaptic gap, the postsynaptic membrane remains in its excited, depolarized state, and transmission of impulses ceases. In effect, the nerves are locked into their "on" state, which is usually fatal to the organism, as acetylcholine is the neurotransmitter for the central

nervous systems of both insects and vertebrates, as well as the neuromuscular and other systems in vertebrates (1).

In the catalytic hydrolysis of acetylcholine, the compound forms an ES complex with acetylcholinesterase, the acyl group is transferred to the enzyme to produce choline, and the unstable acetylated enzyme is rapidly hydrolyzed to acetic acid and regenerated acetylcholinesterase. Organophosphate esters also form ES complexes with the enzyme, with a phosphoryl group being transferred to the enzyme. However, phosphorylated acetylcholinesterase is about 10^7 times less susceptible to hydrolysis than the acetylated enzyme, preventing rapid regeneration of acetylcholinesterase and resulting in irreversible inhibition. The phosphorylation of the enzyme is similar in mechanism to the alkaline hydrolysis of organophosphorus esters, both featuring an S_N2 nucleophilic attack on the phosphorus atom, which bears a partial positive charge. Replacement of the P=S moiety by P=O, because of oxygen's greater electronegativity, increases the positive charge on phosphorus and favors nucleophilic attack, increasing the rate of alkaline hydrolysis (1-2). As expected by analogy, P=O organophosphorus pesticides are several orders of magnitude more active than their P=S counterparts (1-2).

A more comprehensive introduction to the history, synthetic and biological chemistry, and reactions of organophosphorus compounds and pesticides may be found in any of several books on these compounds (1-13), the most recent and comprehensive of which is the treatise by Eto (1).

To realize the goals of this project, ^{31}P nmr was chosen as the main instrumental technique. It is a non-destructive method which allows continuous monitoring of the original pesticide and all phosphorus-containing degradation products. The ^{31}P nucleus, with a spin of $1/2$, 100% natural abundance, relatively high sensitivity (0.0663, relative to ^1H), and large chemical shift range, has very favorable nmr properties. The large ^{31}P chemical shift range and the occurrence of only one phosphorus atom per pesticide molecule result in relatively uncomplicated spectra, from which identification of compounds and measurements of individual resonance areas are straightforward. The disadvantages of using ^{31}P nmr include its poor detection sensitivity, in comparison to techniques such as gas chromatography and infrared or ultraviolet spectroscopy; the fact that only phosphorus-containing species can be monitored; and the limited accuracy of kinetic measurements because of uncertainties in measured peak areas (5-10% at best), low sensitivity, and differential saturation of resonances due to different and relatively long relaxation times.

The majority of nmr studies of organophosphorus pesticides have utilized the ^1H nucleus (15-28, and references therein). Use of ^{31}P has been less frequent. Muller and Goldensen (29), using ^{31}P nmr, determined that a possible catalytic effect was responsible for the intermediacy of the kinetics between zero- and first-order for the isomerization of Systox to Isosystox. The thermal decomposition of Baytex has been followed by ^{31}P nmr (30). Ross and Biros (31) correlated ^{31}P chemical shifts with structure types for thirty-seven pesticides in nine classes of compounds. Gurley and Ritchey (32) analyzed ^{31}P relaxation behavior of several pesticides and related compounds in the

presence of various relaxation reagents. Chemical shifts and relaxation times have been recorded for both pesticides and derivatives, as well as other organophosphorus compounds (33-38, and references therein). This survey is by no means either comprehensive or representative; the interested reader should consult the literature for further references.

B. Experimental

1. Chemicals

The following reference standards were obtained from the Environmental Protection Agency, Perrine, Florida: diazinon (93%), #2080, lot 3179; mevinphos (64.5%), #4640, lot 3285; malathion (99.3%), #4260, lot 3227; methyl parathion (99.9%), #4580, lot 3264; ethyl parathion (99.5%), #5245, lot 3267.

The following were obtained from Chemagro, a division of Baychem Corporation, Kansas City, Missouri: baytex, technical grade; guthion, 93%; and dylox, 98%. Diazinon (92.5%) and supra-cide (99.6%) were obtained from the Geigy Chemical Corporation, Ardsley, New York. Dr. J. Phillips of the Department of Entomology, University of Arkansas, Fayetteville, provided samples of methyl parathion (99+%) and ethyl parathion (99+%), and arranged the procurement of the other pesticides.

Water was double-distilled and deionized before use. Spectrophotometry grade methanol from Baker Chemical Company was used without further purification. Perchloric acid (70%, reagent grade) was obtained from Allied Chemical Company; phosphoric acid (85%,

technical grade) was procured from Fisher.

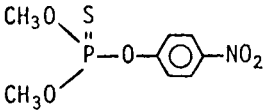
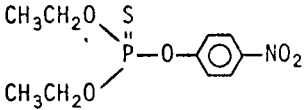
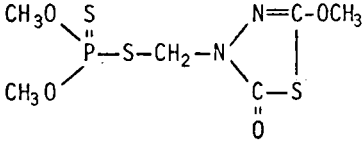
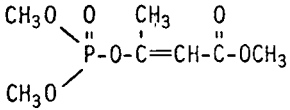
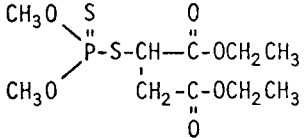
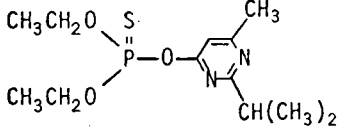
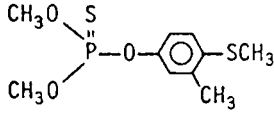
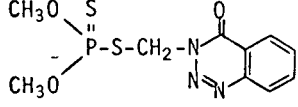
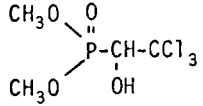
Table 1 lists structures, common and/or trade names, and IUPAC names for the organophosphorus pesticides listed above.

2. Sample Preparation

The pesticide samples were prepared by weight in 5 mm thick-walled nmr tubes to give concentrations of 0.16 ± 0.01 M. This required about 2 mg of pesticide per sample. An aqueous solution of 1.68 mM Cr^{3+} , as $\text{CrCl}_3 \cdot 6\text{H}_2\text{O}$, was added to methanol to form a mixture containing 0.71 ± 0.02 mole fraction methanol, which corresponds to 81.0% MeOH (w/w) or 84.5% MeOH (v/v). The initial pH of this solution was measured and found to be 4.7. A ^{31}P reference compound, dilute aqueous $\text{P}(\text{OH})_4^+$ (39), was sealed in capillary tubes. One of these was placed in each of the nmr tubes, which were then flame-sealed.

The nmr tubes were then placed in Sargent-Welsh constant temperature baths maintained at 60°, 70°, or 90°C, $\pm 0.02^\circ$. Oil was used as the heating fluid for the 90° bath; water was used for the other two. Water-filled test tubes capped with single-hole cork stoppers were immersed in the baths to hold the nmr tubes. At various time intervals, the nmr tubes were removed from the test tubes, quenched in ice water before acquisition of ^{31}P spectra, and afterwards replaced. Assuming a doubling of reaction rate for every 10° temperature increase, a small time correction factor was added to the total elapsed bath immersion time to correct for the elapsed time in the probe during spectral accumulation. Compared to rates at the bath temperatures, reaction rates at the

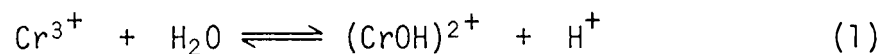
Table 1. Structures and Nomenclature for Some Organophosphorus Pesticides.

Structure	Common Names	IUPAC Name
	methyl parathion, metacide, nitrox	0,0-dimethyl p-nitro- phenyl phosphorothionate
	ethyl parathion, parathion, folidol, thiophos, E605, parafos, rhodiatox	0,0-diethyl p-nitro- phenyl phosphorothionate
	supracide, methida- thion, ustracide, ultracide	0,0-dimethyl S-(2- methoxy-1,3,4-thiadiazol- 5(4H)-onyl-4-methyl) phosphorothiolothionate
	mevinphos, phosdrin	0,0-dimethyl 1-methoxy- carbonyl-1-propene-2- yl phosphate
	malathion, cythion, karbofos, pencathion	S-[1,2-di(ethoxycarbonyl) ethyl] 0,0-dimethyl phosphorothiolothionate
	diazinon, basudin, srolex, exodin, sarolex	0,0-diethyl 2-isopropyl- 6-methyl-4-pyrimidinyl phosphorothionate
	baytex, fenthion, lebaycid, entex, tiguvon, S 1752	0,0-dimethyl 3-methyl- 4-methylthiophenyl phosphorothionate
	guthion, gusathion, azinhosmethyl, methyl gusathion	0,0-dimethyl S-(4-oxo- 1,2,3-benzotriazin-3(4H)- ylmethyl) phosphorothio- thionate
	dylox, trichlorfon, phoschlor, trichlorphon, metrifonate, chlorophos, dipterex, neguvon, tugon, soldep	0,0-dimethyl 1-hydroxy- 2,2,2-trichloroethyl phosphonate

probe temperature are so slow that this correction factor could have been omitted without introducing appreciable error.

3. Acquisition of Spectra

Due to the long relaxation times of ^{31}P , which can be 30s or more, paramagnetic Cr^{3+} was added as a relaxation reagent to shorten the T_1 values and permit more rapid pulsing, without loss of signal-to-noise as a result of saturation. The arbitrarily-selected amount of added Cr^{3+} corresponds to a 600:1 pesticide: Cr^{3+} molar ratio; the initial molar ratios of all the sample components were $\text{MeOH:H}_2\text{O:pesticide:Cr}^{3+} = 81000:33000:600:1$. Adding Cr^{3+} to water changes the pH due to the hydrolysis reaction



The equilibrium constant for this hydrolysis is 1.5×10^{-4} (40). Since the solvent for the pesticides was aqueous methanol rather than water, the pH could not be calculated, so was determined empirically.

The data acquisition parameters were as follows: pulse angle, 75° ; pulse repetition time, 2 s; spectral window, 4 kHz; number of frequency-domain data points, 4k; line-broadening from exponential weighting of FID, 2.5 Hz; number of transients accumulated, about 1000. The probe temperature was about 24°C . At the field strength used, 21.14 kG, ^{31}P resonates at about 36.43 MHz.

The ^1H lock signal was provided by the MeOH methyl protons of the aqueous methanol solvent. Measurements of the resonance frequencies of 85% H_3PO_4 , of 10% aqueous trimethyl phosphate, $(\text{MeO})_3\text{PO}$, and of the dilute sample of $\text{P}(\text{OH})_4^+$ in a capillary immersed in a tube of the aqueous methanol solvent were made. Corrected to a field in which the protons of TMS resonate at exactly 100 MHz, the frequencies (ν/MHz) are 40.480824 for $(\text{MeO})_3\text{PO}$, 40.480718 for $\text{P}(\text{OH})_4^+$ in the capillary, and 40.480703 for H_3PO_4 . The H_3PO_4 value can be compared to that of 40.480790 MHz reported by others (41) for $\nu(^{31}\text{P})$ of 85% H_3PO_4 . These frequencies were used to determine the chemical shifts of 10% aqueous $(\text{MeO})_3\text{PO}$, +3.13 ppm, and of external $\text{P}(\text{OH})_4^+$, +0.36 ppm, with respect to 85% H_3PO_4 . Positive values denote high-frequency (low-field) shifts, in accordance with IUPAC convention, the reverse of the tradition followed in reporting ^{31}P shifts in the past. Chemical shifts were measured with respect to the external $\text{P}(\text{OH})_4^+$ signal as secondary reference, and then converted to values with respect to the primary reference of 85% H_3PO_4 by adding +0.36 ppm to the measured chemical shifts. The primary purpose of the $\text{P}(\text{OH})_4^+$ was to serve as a standard in the measurement of relative signal areas; all ^{31}P integrated peak intensities were normalized to that of the phosphonium ion as unity. The areas were measured as the average of at least three integrated signal traces; errors are estimated to be $\pm 5\%$ to $\pm 10\%$. Spectra were obtained without broadband ^1H decoupling in order to make identification of compounds easier.

C. Results and Discussion

Representative chemical shift ranges of various types of organophosphorus compounds are given in Table 2. This and more comprehensive tabulations (15-16, 29-32, 38) proved invaluable in assigning resonances.

1. Ethyl Parathion

Figure 1 shows a selected series of spectra taken during the degradation of ethyl parathion. The parent pesticide, at +62.15 ppm, is first hydrolyzed to $\text{SPO}(\text{OEt})_2^-$, at +64.0 ppm. A compound, as yet not positively identified, then appears at +53.05 ppm, followed by the phosphates $\text{OPO}(\text{OEt})_2^-$, $\text{OPO}(\text{OH})(\text{OEt})^-$, and $\text{OPO}(\text{OH})_2^-$ at 0 to +4 ppm. (The degree of protonation of all hydrolysis products was assumed by comparison with the phosphate system, which exists as nearly 100% diprotonated monoanion at pH 4.7 (38,42).) Next to appear is a peak at +65.4 ppm, which is probably $\text{SPO}(\text{OH})(\text{OEt})^-$, from hydrolysis of an ethoxy group of $\text{SPO}(\text{OEt})_2^-$. At 60° and 70°, this resonance did not appear until after about five weeks and three weeks, respectively, had elapsed, consistent with the fact that phosphate diesters are much less inclined to hydrolyze than are monoesters or triesters (1). Traces of compounds with chemical shifts of +32.6 ppm and +16.4 ppm were also noted, especially at 90°. The +32.6 ppm signal is probably from the phosphorothiolate isomerization product $\text{OPO}(\text{OEt})(\text{SEt})^-$, although the chemical shift is also consistent with a phosphonate, such as $\text{OP}(\text{Et})(\text{OEt})_2$. Thiono-thiolo isomerization usually requires temperatures of about 100°C (1). The +16.4 ppm resonance occurs in the region expected for the phosphonate

Table 2. ^{31}P Chemical Shifts of Some Phosphorus Compounds.^{a,b}

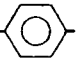
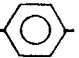
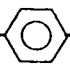
Compound	$\delta(^{31}\text{P})/\text{ppm}$	W	X	Y	Z
<u>Phosphates</u>	-2 to +6	0	0	0	0
OP(OH) ₃	0.0				
OPO(OH) ₂ ⁻	+0.3 to +0.5				
OPO ₂ (OH) ²⁻	+3.1 to +3.3				
OPO ₃ ³⁻	+5.4 to +6.0				
OP(OR) ₃	-2.4 to +2.5	(R = Me, Et)			
OP(OPh) ₃	+18				
OPO(OEt) ₂ ⁻	+2.8 to +3.8				
<u>Phosphorothiolates</u>	+22 to +32	0	0	S	0
OP(OMe) ₂ (SPr ⁿ)	+31				
OP(OEt) ₂ (SR)	+26.4 to +28.6	(R=Me, Et, Pr ⁿ , Bu ⁿ)			
OP(OEt) ₂ (SPh)	+22				
OP(OMe)(O-  -NO ₂)(SR)	+24.0 to +25.2	(R = Me, Et)			
OPS(OR) ₂ ⁻	+24.0	(R = Et, Bu ^t)			
OPSO ₂ ³⁻	+31.0 to +33.8				
<u>Phosphorodithiolates</u>	+50 to +62	0	S	S	0
OP(OEt)(SEt) ₂	+53.5				
OPOS ₂ ³⁻	+61 to +62				
<u>Phosphorothionates</u>	+55 to +70	0	0	0	S
SP(OMe) ₃	+73				
SP(OR) ₃	+65 to +70	(R=Et, Pr ⁿ , Bu ^t)			
SP(OR) ₂ (O-  -NO ₂)	+62 to +65 ^c	(R = Me, Et)			
SP(OPh) ₃	+53.4				
<u>Phosphorodithionates</u>	+85 to +105	0	0	S	S
SP(OR) ₂ (SR)	+91 to +100	(R=Me, Et, Pr ⁱ)			
SP(OMe) ₂ (SPh)	+90				
SP(OR) ₂ (SH)	+82 to +86	(R=Et, Pr ⁱ , Bu ⁿ)			
SPS(OR) ₂ ⁻	+107 to +111	(R = Et, Pr ⁱ)			

Table 2.

<u>Compound</u>	<u>$\delta(^{31}\text{P})/\text{ppm}$</u>	<u>W</u>	<u>X</u>	<u>Y</u>	<u>Z</u>
<u>Phosphorotriithiolates</u>	+60 to +85	S	S	S	0
OP(SMe) ₃	+66 to +67				
OP(SR) ₃	+61 to +63	(R=Et, Pr ⁿ , Bu ⁿ)			
OP(SBu ^t) ₃	+85.2				
OP(SPh) ₃	+55.2				
OPS ₃ ³⁻	+86				
<u>Thiophosphates</u>	+88 to +98	S	S	S	S
SP(SMe) ₃	+98				
SP(SR) ₃	+91 to +93	(R=Et, Pr ⁿ , Bu ⁿ , Ph)			
SPS ₃ ³⁻	+87 to +88				
<u>Phosphonothionates</u>	+80 to +95	0	0	C	S
SP(Me)(OEt) ₂	+94.9				
SP(Me)(OEt)(O-  -NO ₂)	+94.3				
SP(Me)(OEt)(OH)	+88.8				
SP(Et)(OEt)(OH)	+94.2				
SP(Me)(OMe) ₂	+80.5				
SPO(Me)(OEt) ⁻	+76.0				
<u>Phosphonates</u>		0	0	C	0
OPR(OR') ₂	+27 to +33	(R=Me, Et, Bu ⁿ ; R'=Me, Et, Pr ⁱ , Pr ⁿ , Bu ⁿ)			
OP(Me)(OR) ₂	+21 to +24	(R=Bu ^t , Ph)			
OP(Ph)(OR) ₂	+16 to +22	(R=Me, Et, Pr ⁱ , Pr ⁿ)			
OP(Ph)(OPh) ₂	+11.2				

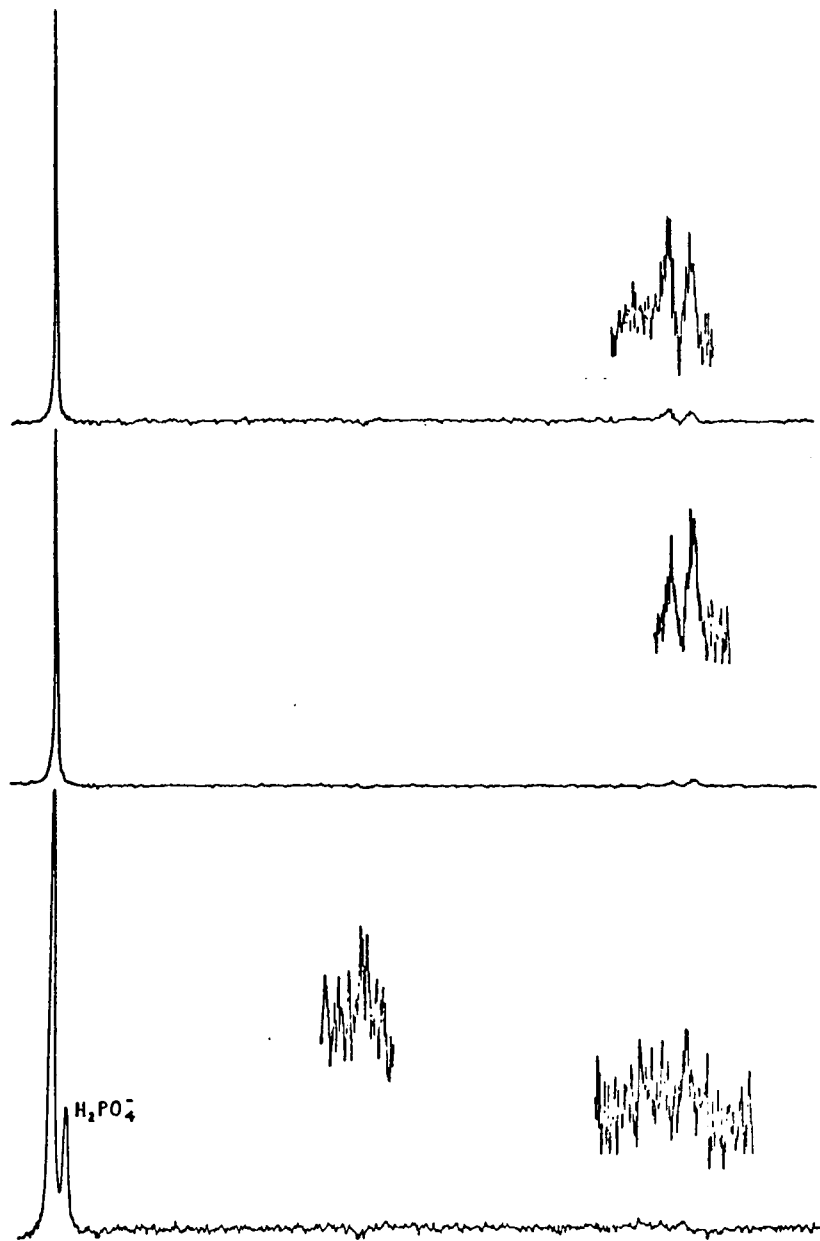
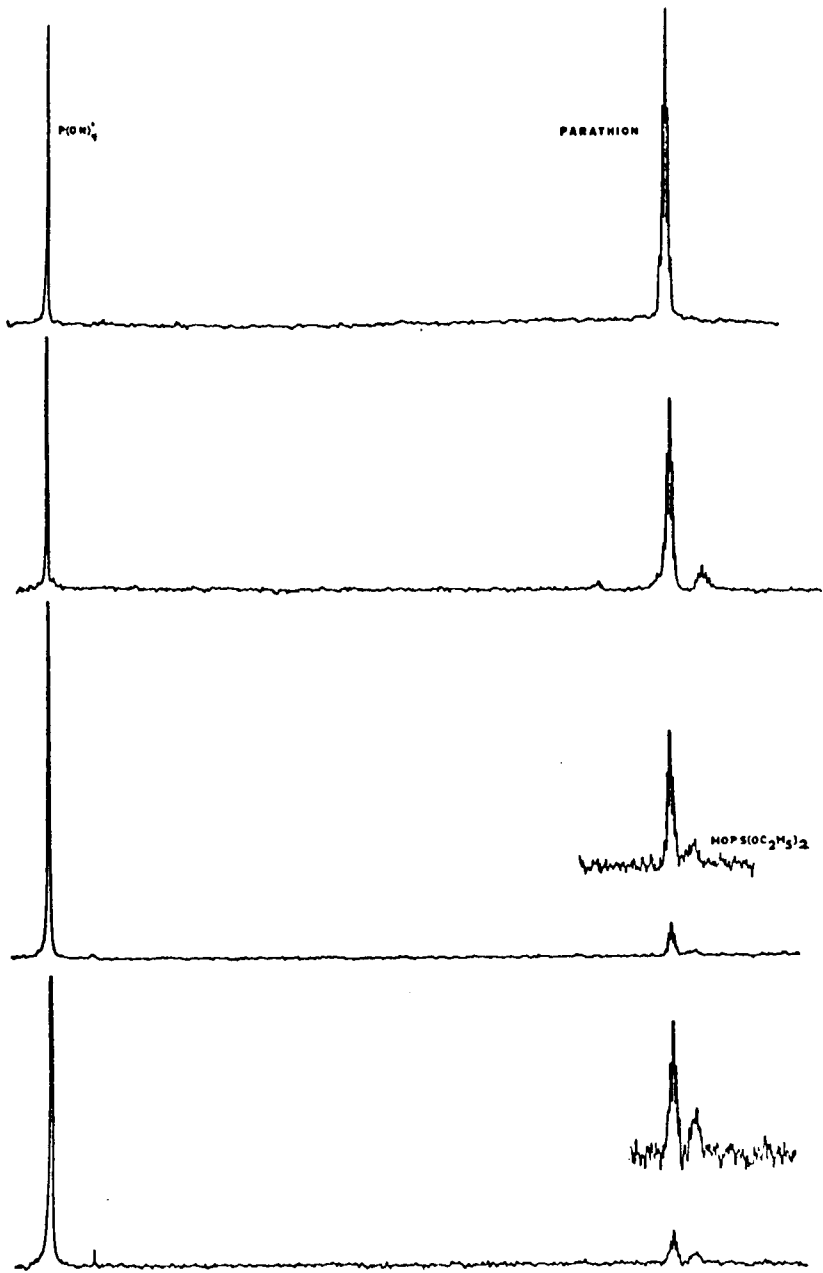
^a From references 31 and 38.

^b Tetra-coordinate, structures of $\text{R}^1\text{W}-\overset{\text{Z}}{\overset{\parallel}{\text{P}}}-\text{YR}^3$, where R¹, R², and R³ are H, alkyl, and/or aromatic.

^c For R=Et, reference 38 incorrectly lists +42 ppm.

FIGURE 1

The degradation of ethyl parathion as monitored by ^{31}P nmr at 36.43 MHz. The field strength B_0 decreases from left to right.



$OP(C_6H_4NO_2)(OEt)_2$. The signal at +53.05 ppm is tentatively assigned to a phosphorodithiolate.

Figures 2-4 show the intensity changes of the ^{31}P signals of ethyl parathion and its degradation products at 60°, 70°, and 90°, as functions of the total elapsed time. Tables 3-5 contain the data in numerical form.

2. Methyl Parathion

Selected ^{31}P spectra showing the degradation of methyl parathion are presented in Figure 5. The methyl parathion ^{31}P resonance occurs at +65.75 ppm. The first product appears at +55.4 ppm, and is probably a phosphorodithiolate. Almost simultaneously, two peaks at +17.0 and +1.5 ppm appear; the +17.0 ppm peak is likely to be $OP(C_6H_4NO_2)(OMe)_2$, and the multiplet at +1.5 ppm is $OPO(OMe)_2^-$, with $^3J(^{31}P^1H) = 11.0 \pm 0.5$ Hz. In some of the spectra a trace of a compound, most likely the thiono-thiolo isomerization product $OPO(OMe)(SMe)^-$, with a chemical shift of about +34 ppm is visible.

The time dependences of the ^{31}P signal areas of methyl parathion and its degradation products at 60° and 70° are plotted in Figures 6 and 7; the data are also presented in Tables 6-8.

3. Supracide

Spectra of the pesticide supracide and its decomposition products are shown in Figure 8. The supracide peak at +95.20 ppm diminishes as a resonance due to $SP(OMe)_2(OH)$ grows at +65.2 ppm. This forms from P-S bond fission (1) as follows:

FIGURE 2

Time course of the degradation of ethyl parathion (circles) at +62.15 ppm and the formation and reaction of the hydrolysis product $\text{PS(OH)(OC}_2\text{H}_5)_2$ (squares) at +64.0 ppm. Temperature was 60°C; initial pH was 4.7.

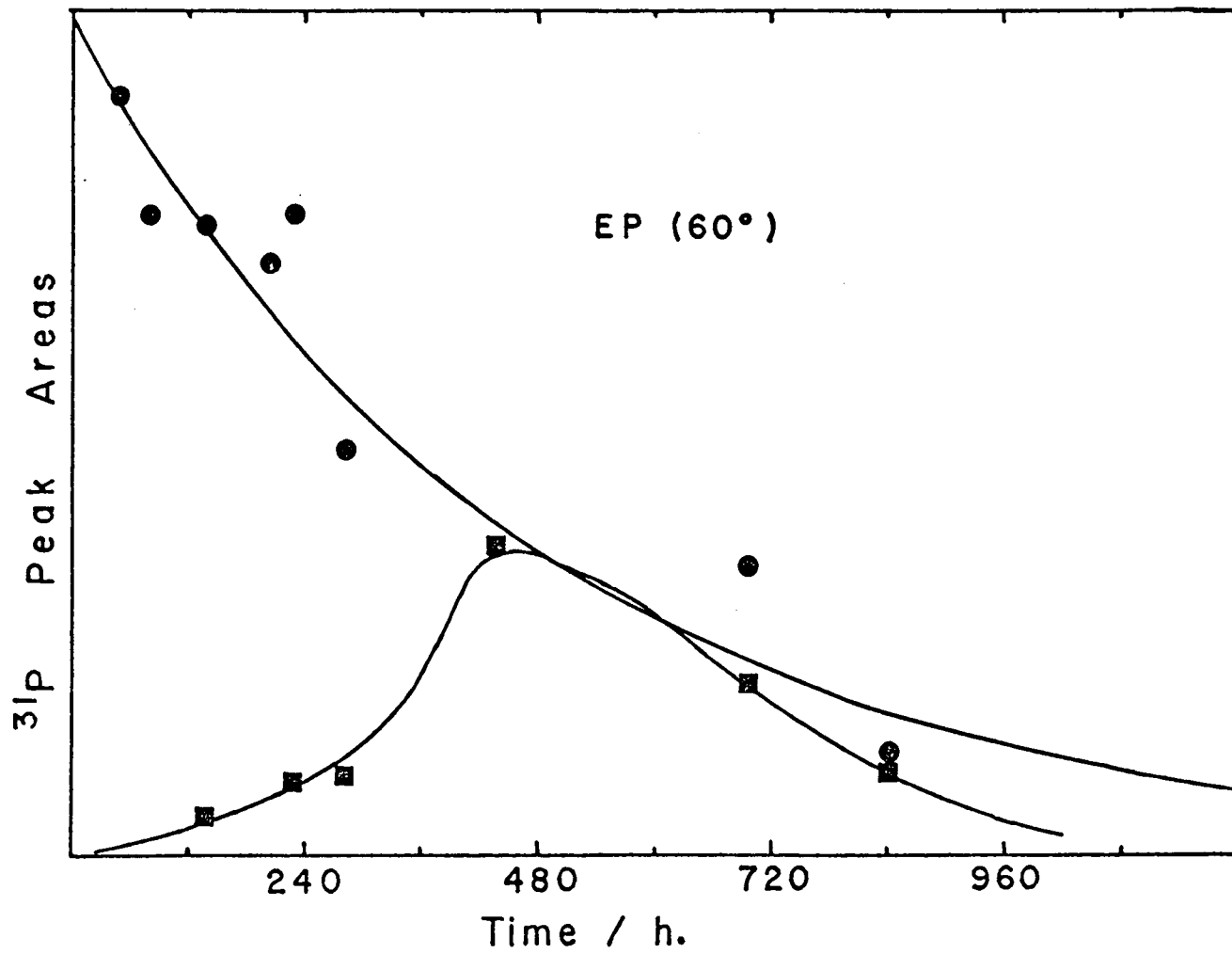


FIGURE 3

Time course of the degradation of ethyl parathion (circles) at +62.15 ppm and the buildup and decay of products at +64.0 ppm (squares), +53.05 ppm (hexagons), and +0.8 to +1.9 ppm (triangles), at 70°C.

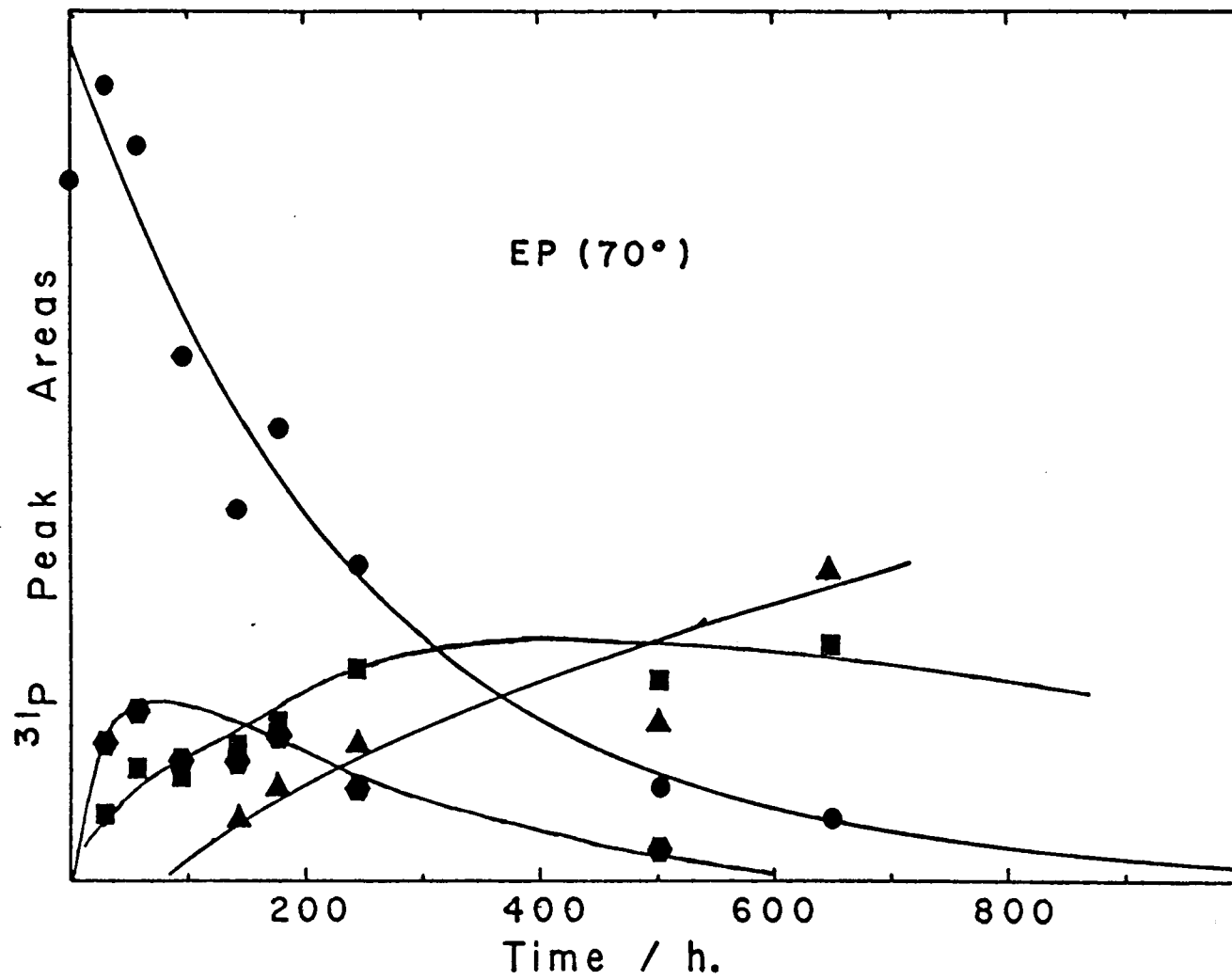


FIGURE 4

The decomposition of ethyl parathion (circles) at +62.15 ppm and the formation and decay of products at +64.0 ppm (squares), +53.05 ppm (hexagons), and +0.8 to +1.9 ppm (triangles), at 90°C. Initial pH was 4.7.

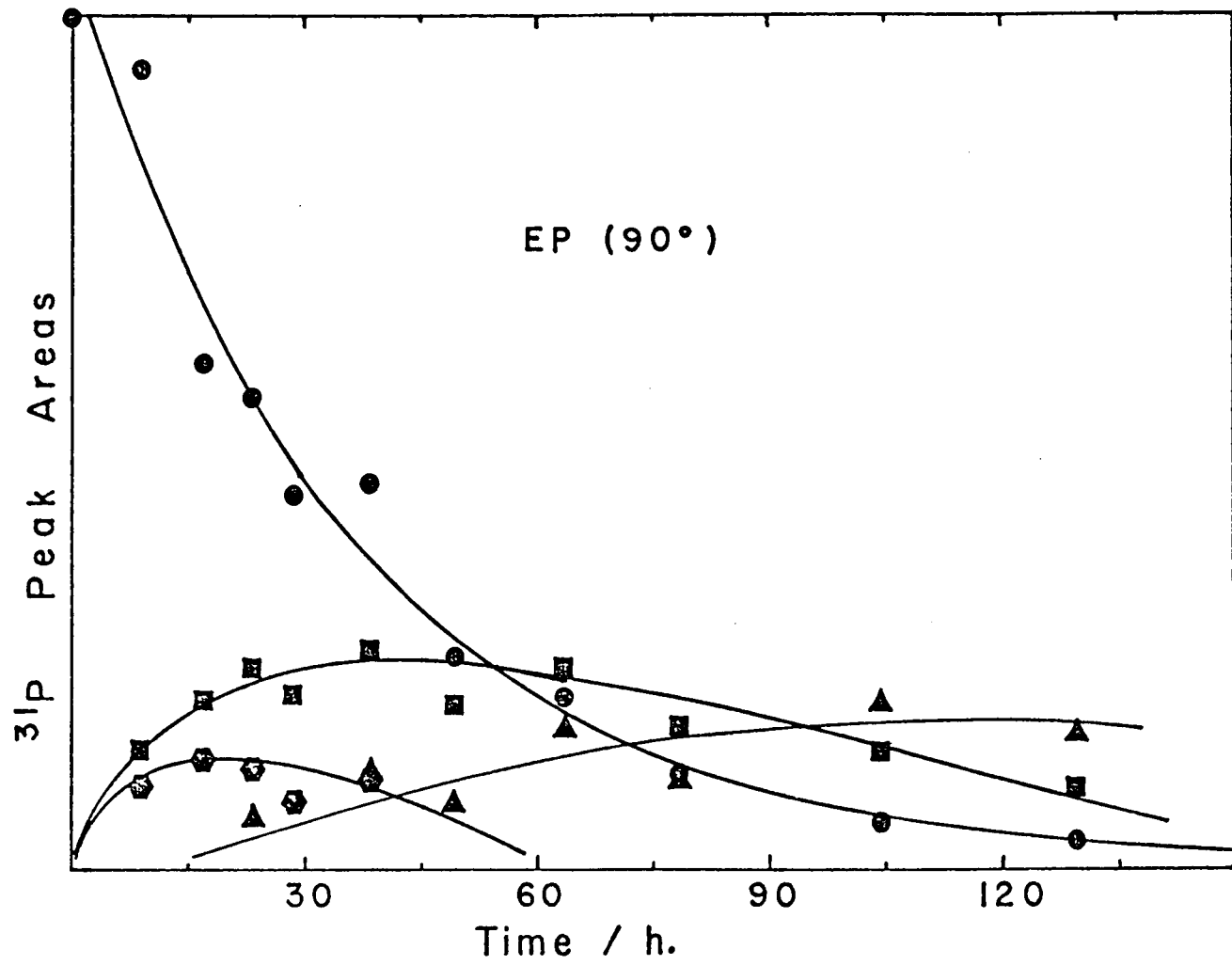


Table 3. Relative ^{31}P Peak Areas of Ethyl Parathion and Its Degradation Products at 60°C.

Time/h	+62.15 ppm ^b	+64.0 ppm ^c	+53.05 ppm ^d	+0.9,+1.8 ppm ^e
0.00				
48.64	3.140			
80.52	2.650			
138.15	2.609			
202.58	2.446	0.160		
230.15	2.646	0.293		
282.29	1.671	0.328		
436.58	2.749	1.272		
695.92	1.185	0.714		0.210
842.26 ^a	0.424	0.343	0.343	0.336
1199.97 ^f	0.767	1.226	0.289	
2614.15 ^g	0.356	0.691		0.666

^a Also a peak at +65.4 ppm, relative area 0.205, probably due to $\text{SPO}(\text{OH})(\text{OEt})^{\ominus}$ and one at -0.6 ppm, relative area 0.164, from a phosphate.

^b Ethyl parathion, $\text{SP}(\text{OEt})_2(\text{O}-\text{C}_6\text{H}_4-\text{NO}_2)$.

^c $\text{SPO}(\text{OEt})_2^{\ominus}$.

^d Probably a phosphorodithiolate.

^e Phosphates.

^f Also a small peak at +16.4 ppm, possibly from a phosphonate.

^g Also a weak signal at +32.6 ppm, possibly due to $\text{OPO}(\text{OEt})(\text{SEt})^{\ominus}$.

Table 4. Relative ^{31}P Peak Areas of Ethyl Parathion and Its Degradation Products at 70°C.

Time/h	+62.15 ppm ^c	+64.0 ppm ^d	+53.05 ppm ^e	+0.9,+1.8 ppm ^f
0.00	2.810			
30.57	3.194	0.268	0.544	
57.69	2.950	0.446	0.673	
95.61	2.101	0.413	0.476	
143.15	1.491	0.537	0.475	0.247
178.04	1.814	0.635	0.578	0.377
245.89	1.266	0.855	0.368	0.538
502.03 ^a	0.378	0.806	0.122	0.631
648.83 ^b	0.257	0.948		1.244
1009.74 ^g	0.162	0.425		1.018
2423.19		0.375		4.242

^a Also a peak at +65.4 ppm, relative area 0.120, probably due to $\text{SPO}(\text{OH})(\text{OEt})^-$, and a weak signal at +32.6 ppm.

^b Also a +65.4 ppm peak with relative area 0.263, probably assignable to $\text{SPO}(\text{OH})(\text{OEt})^-$, plus a -0.6 ppm signal, with relative area 0.542, from a phosphate.

^c Ethyl parathion, $\text{SP}(\text{OEt})_2(\text{O}-\text{C}_6\text{H}_4-\text{NO}_2)$.

^d $\text{SPO}(\text{OEt})_2^-$.

^e Probably a phosphorodithiolate.

^f Phosphates.

^g Also a phosphate peak at -0.6 ppm, relative area 0.387.

Table 5. Relative ³ Peak Areas of Ethyl Parathion and Its Degradation Products at 90°C.^{f,g}

Time/h	+62.15 ppm ^a	+64.0 ppm ^b	+53.05 ppm ^c	+0.9,+1.8 ppm ^d	+65.4 ppm ^e
0.00	3.195				
12.01	3.467	0.506	0.618		
31.15	2.267	0.912	0.258		
72.29	0.815	0.867		0.376	
90.27	0.685	0.833		0.334	
96.46	0.579	0.965		0.763	
117.62	0.346	0.841		0.630	
139.96	0.067	0.255		0.801	
168.89	0.072	0.427		1.151	
217.90	0.421	0.674		1.260	
1812.74				1.694	
0.00	4.182				
9.06	3.937	0.576	0.405		
16.94	2.478	0.822	0.530		0.328
23.36	2.299	0.984	0.490	0.249	
28.67	1.833	0.854	0.328	0.325	0.277
38.44	1.888	1.071	0.446	0.469	0.696
49.33	1.041	0.801		0.311	0.367
63.47	0.842	0.989		0.682	0.237
78.40	0.478	0.693		0.431	0.226
104.41	0.224	0.571		0.808	0.210
129.54	0.133	0.389		0.658	0.087

Table 5.

^a Ethyl parathion, $\text{SP}(\text{OEt})_2(\text{O}-\text{C}_6\text{H}_4-\text{NO}_2)$.

^b $\text{SP}(\text{OEt})_2^-$.

^c Probably a phosphorodithiolate.

^d Phosphates.

^e Probably $\text{SP}(\text{OH})(\text{OEt})^-$.

^f A phosphate peak at +4.3 ppm occurred at the following times, with the corresponding relative areas: 9.06 h, 0.185; 16.94 h, 0.383; 38.44 h, 0.473. A -0.6 ppm phosphate signal was observed also: 117.62 h, 0.188; 139.96 h, 0.182; 168.89 h, 0.066; 217.90 h, 0.633; 1812.74 h, 0.803; 78.40 h, 0.034; 104.41 h, 0.094; 129.54 h, 0.204.

^g Also a weak signal, possibly due to $\text{OP}(\text{OEt})(\text{SEt})^-$, at +32.6 ppm, at 139.96 h, 168.89 h, and 217.90 h.

FIGURE 5

The degradation of methyl parathion as monitored by ^{31}P nmr at 36.43 MHz. The field strength B_0 decreases from left to right.

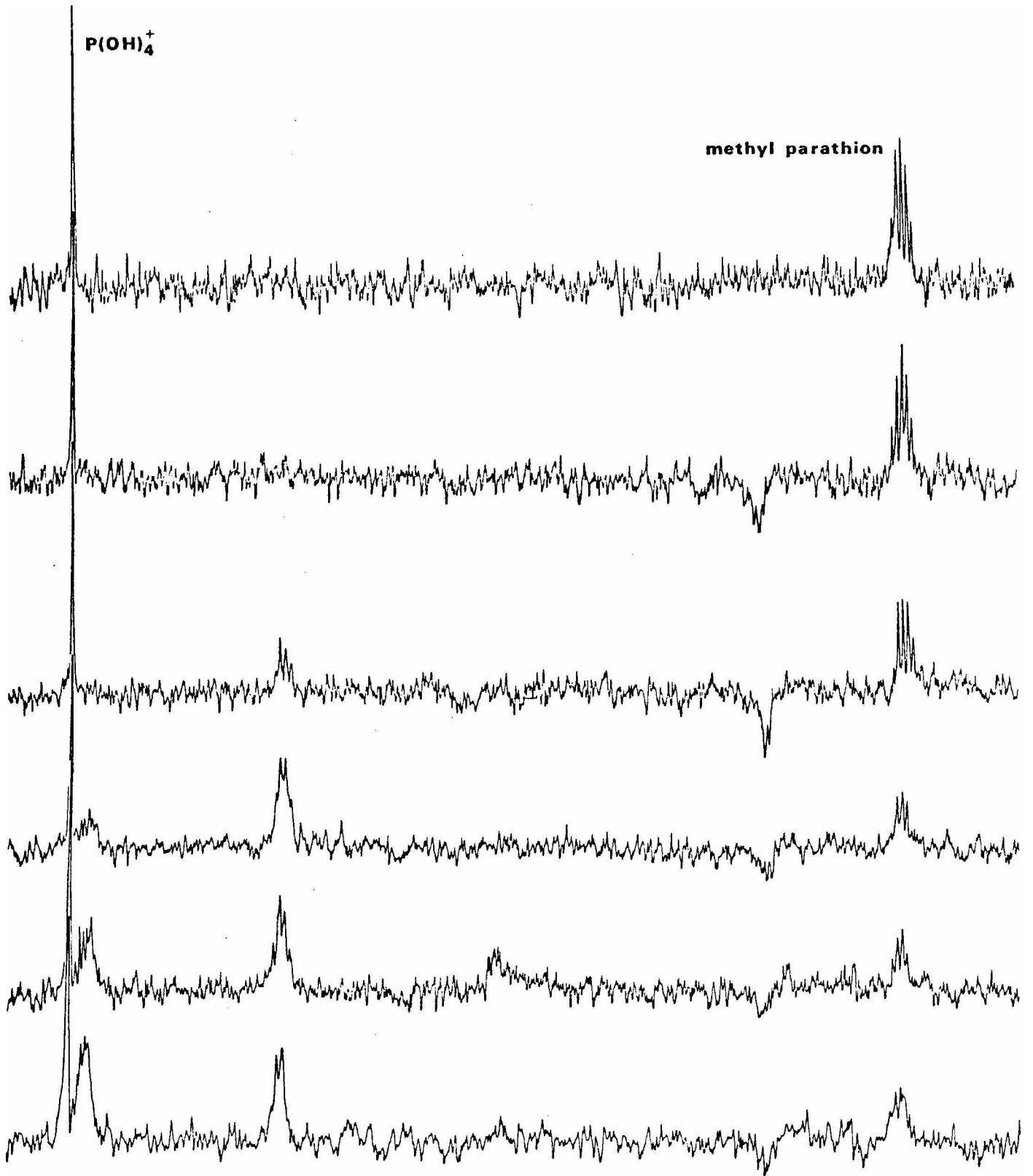
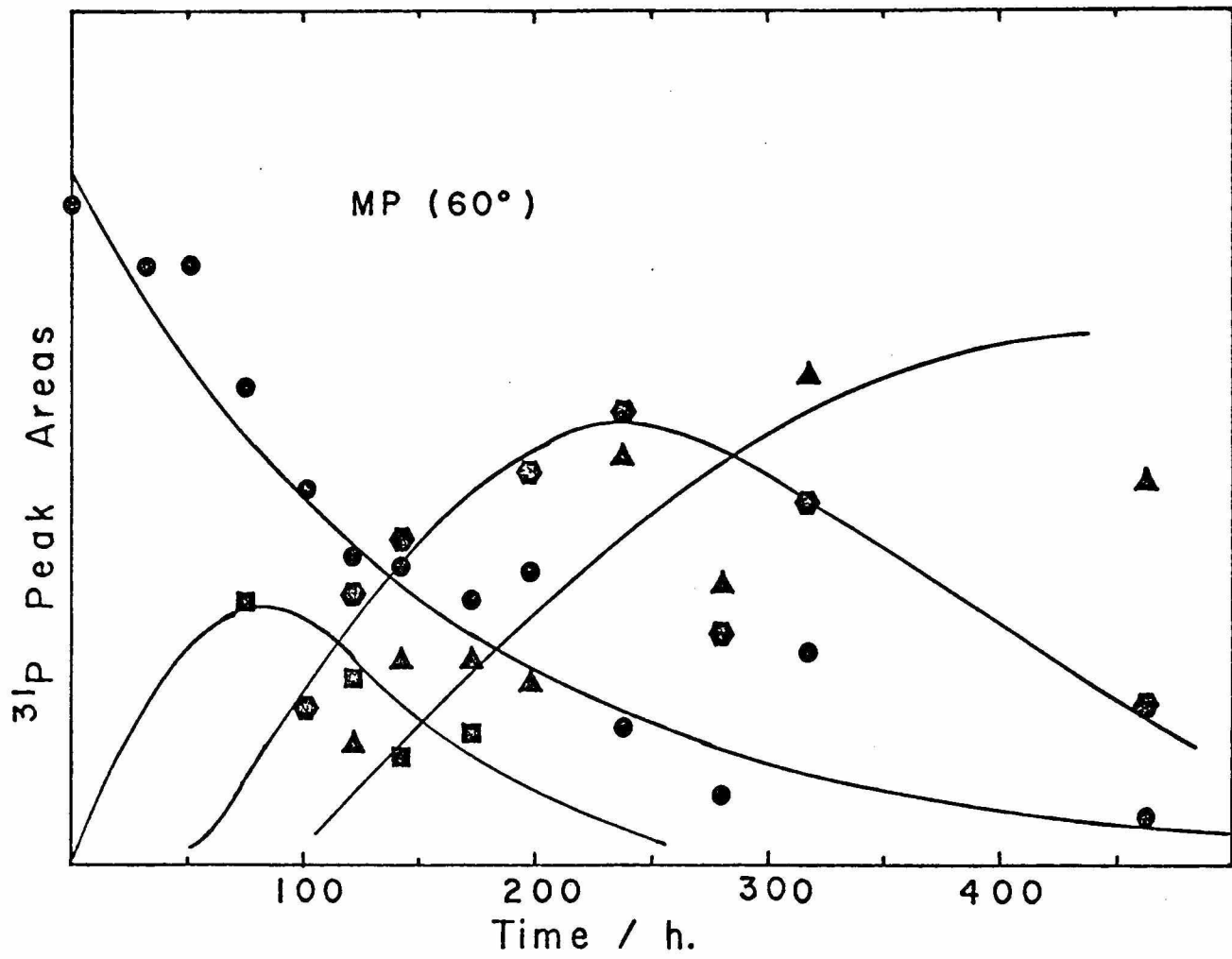


FIGURE 6

Plot of relative ^{31}P peak areas vs. time for methyl parathion (circles) at +65.75 ppm, and for degradation products at +55.4 ppm (squares), +17.0 ppm (hexagons), and +1.5 ppm (triangles). Temperature was 60°C ; initial pH was 4.7.



· FIGURE 7

Relative ^{31}P peak areas as functions of time for methyl parathion (circles) at +65.75 ppm, and for degradation products at +55.4 ppm (squares), +17.0 ppm (hexagons), and +1.5 ppm (triangles). Temperature was 70° ; initial pH was 4.7.

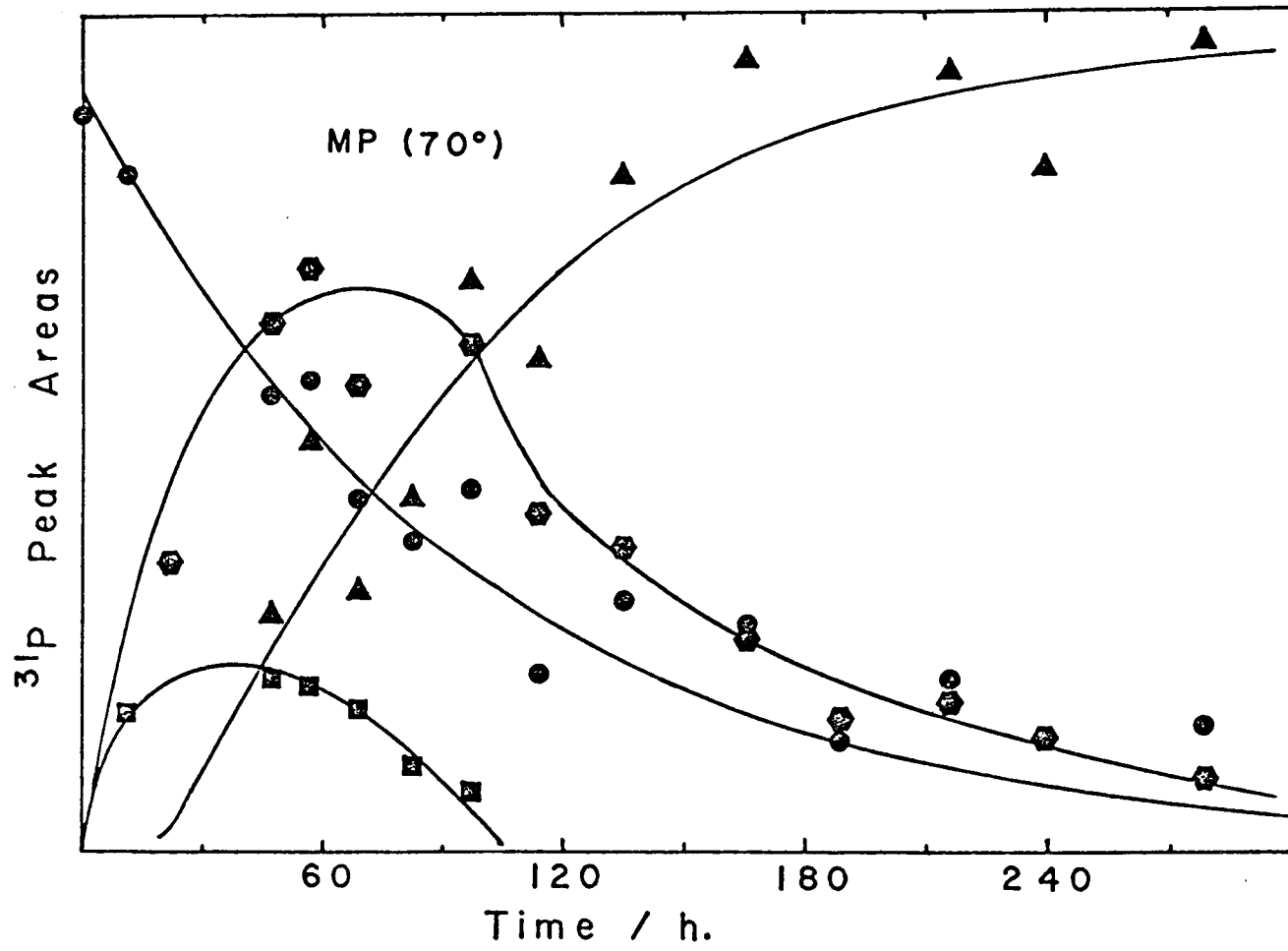


Table 6. Relative ^{31}P Peak Areas of Methyl Parathion and Its Degradation Products at 60°C .^e

Time/h	+65.75 ppm ^a	+55.4 ppm ^b	+17.0 ppm ^c	+1.5 ppm ^d
0.00	2.695			
31.90	2.442			
50.90	2.449			
75.10	1.952	1.064		
101.85	1.533		0.635	
121.76	1.257	0.745	1.092	0.488
142.56	1.208	0.438	1.328	0.829
172.98	1.075	0.529	1.053	0.833
198.12	1.190		1.595	0.738
238.12	0.560		1.847	1.659
280.29	0.279		0.936	1.141
317.21	0.865		1.473	1.987
462.73	0.189		0.651	1.559
1517.00				2.695

^a Methyl parathion, $\text{SP}(\text{OMe})_2(\text{O}-\text{C}_6\text{H}_4-\text{NO}_2)$.

^b Probably a phosphorodithiolate.

^c Probably $\text{OP}(\text{C}_6\text{H}_4\text{NO}_2)(\text{OMe})_2$.

^d Phosphates, mostly $\text{OPO}(\text{OMe})_2^-$.

^e In some spectra, a small peak at +34 ppm, possibly arising from $\text{OPO}(\text{OMe})(\text{SMe})^-$, was observed.

Table 7. Relative ^{31}P Peak Areas of Methyl Parathion and Its Degradation Products at 70°C .^e

Time/h	+65.75 ppm ^a	+55.4 ppm ^b	+17.0 ppm ^c	+1.5 ppm ^d
0.00	3.091			
11.30	2.843	0.568		
21.95	3.463		1.194	
47.38	1.910	0.713	2.197	0.976
56.76	1.975	0.685	2.432	1.706
69.24	1.477	0.586	1.938	1.078
83.02	1.305	0.352	1.564	1.466
97.59	1.516	0.250	2.108	2.383
114.07	0.754		1.398	2.055
135.43	1.045		1.258	2.818
165.80	0.942		0.872	3.310
188.87	0.466		0.504	1.796
215.83	0.723		0.613	3.254
239.36	0.885		0.466	2.845
278.63	0.522		0.299	3.372
1303.46				3.005

^a Methyl parathion, $\text{SP}(\text{OMe})_2(\text{O}-\text{C}_6\text{H}_4-\text{NO}_2)$.

^b Probably a phosphorodithiolate.

^c Probably $\text{OP}(\text{C}_6\text{H}_4\text{NO}_2)(\text{OMe})_2$.

^d Phosphates, mostly $\text{OPO}(\text{OMe})_2^-$.

^e In some spectra, a small peak at +34 ppm, probably arising from $\text{OPO}(\text{OMe})(\text{SMe})^-$, was observed.

Table 8. Relative ^{31}P Peak Areas of Methyl Parathion and Its Degradation Products at 90°C .^e

Time/h	+65.75 ppm ^a	+55.4 ppm ^b	+17.0 ppm ^c	+1.5 ppm ^d
0.00	2.805			
13.38	1.288	0.375	1.077	1.119
18.47	1.216		1.185	1.280
25.25	0.779		0.753	1.645
34.63	0.835		0.203	1.747
41.25	0.650			2.075
52.38	0.505			2.697
66.29	0.371			2.143
74.02	0.294			1.839
103.20	0.328			2.327
127.89	0.236			2.373
156.27	0.286			2.273
200.28	0.323			2.189
237.82	0.190			2.322
1802.48				1.353
0.00	2.653			
3.06	1.897	0.337		
6.70	1.519	0.419	0.884	
8.11	1.805	0.379	0.974	
9.84	1.365		0.906	0.495
16.11	0.917		0.954	0.631
21.81	1.049	0.364	0.680	1.298
31.89	0.938		0.383	1.843
51.90	0.524			1.354
70.99	0.305			2.113
84.38	0.288			1.445
107.09	0.231			1.736
130.47	0.370			2.396
1720.15				1.250

^a Methyl parathion, $\text{SP}(\text{OMe})_2(\text{O}-\text{C}_6\text{H}_4-\text{NO}_2)$.

^b Probably a phosphorodithiolate.

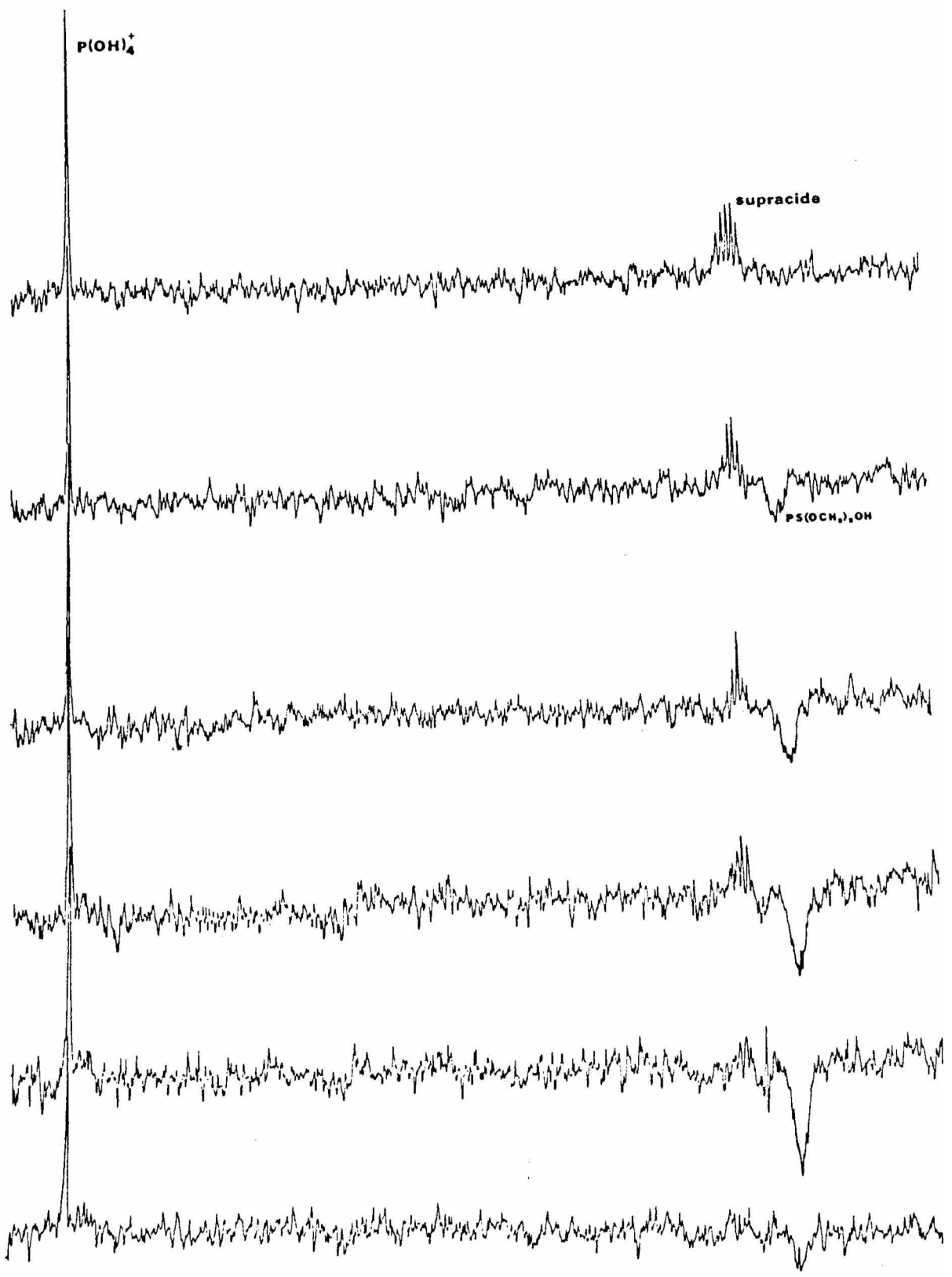
^c Probably $\text{OP}(\text{C}_6\text{H}_4\text{NO}_2)(\text{OMe})_2$.

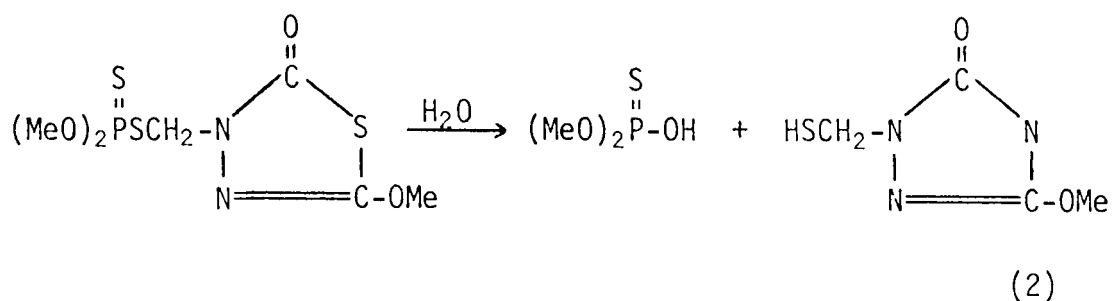
^d Phosphates, mostly $\text{OPO}(\text{OMe})_2^-$.

^e In some spectra, a small peak at +34 ppm, probably arising from $\text{OPO}(\text{OMe})(\text{SMe})^-$, was observed.

FIGURE 8

The degradation of supracide as monitored by ^{31}P nmr at 36.43 MHz. The field strength B_0 decreases from left to right. The supracide peak is folded from the high-frequency side of the spectral window.





The second supracide product, which is found at +34.2 ppm, is undoubtedly $\text{OP}(\text{OMe})(\text{OH})(\text{SMe})$, formed by thiono-thiolo isomerization of the first product. Next to appear are the phosphates, at +1.85 ppm. Signals also appear at +100.0 ppm and, especially at 90° , at +61.8 ppm; the former is probably due to the phosphorodithionate $\text{SP}(\text{OMe})_2(\text{SMe})$, and the latter is assigned to $\text{SPO}(\text{OMe})(\text{OH})^-$, the hydrolysis product of the first intermediate formed. A small signal at about +24.9 ppm appears in a few of the spectra, indicative of a phosphorothiolate, and undoubtedly formed by thiono-thiolo isomerization.

Figures 9 and 10 are plots of ^{31}P peak areas as a function of time for supracide and its phosphorus-containing products at 60° and 90° , taken from the data in Tables 9-11.

4. Summary

The hydrolysis reactions are expected to be second order, dependent on the concentrations of solvent and of pesticide (1). However, since the solvent concentration was much greater than that of the pesticide, pseudo-first-order kinetics were assumed, described by the rate equation

$$d[\text{pesticide}]/dt = -k[\text{pesticide}] \quad (3)$$

FIGURE 9

Time-dependence of the ^{31}P peak areas during the degradation of supracide (circles) at +95.20 ppm to products at +65.2 ppm (squares), +34.2 ppm (hexagons), and +1.85 ppm (triangles). Temperature was 60° ; initial pH was 4.7.

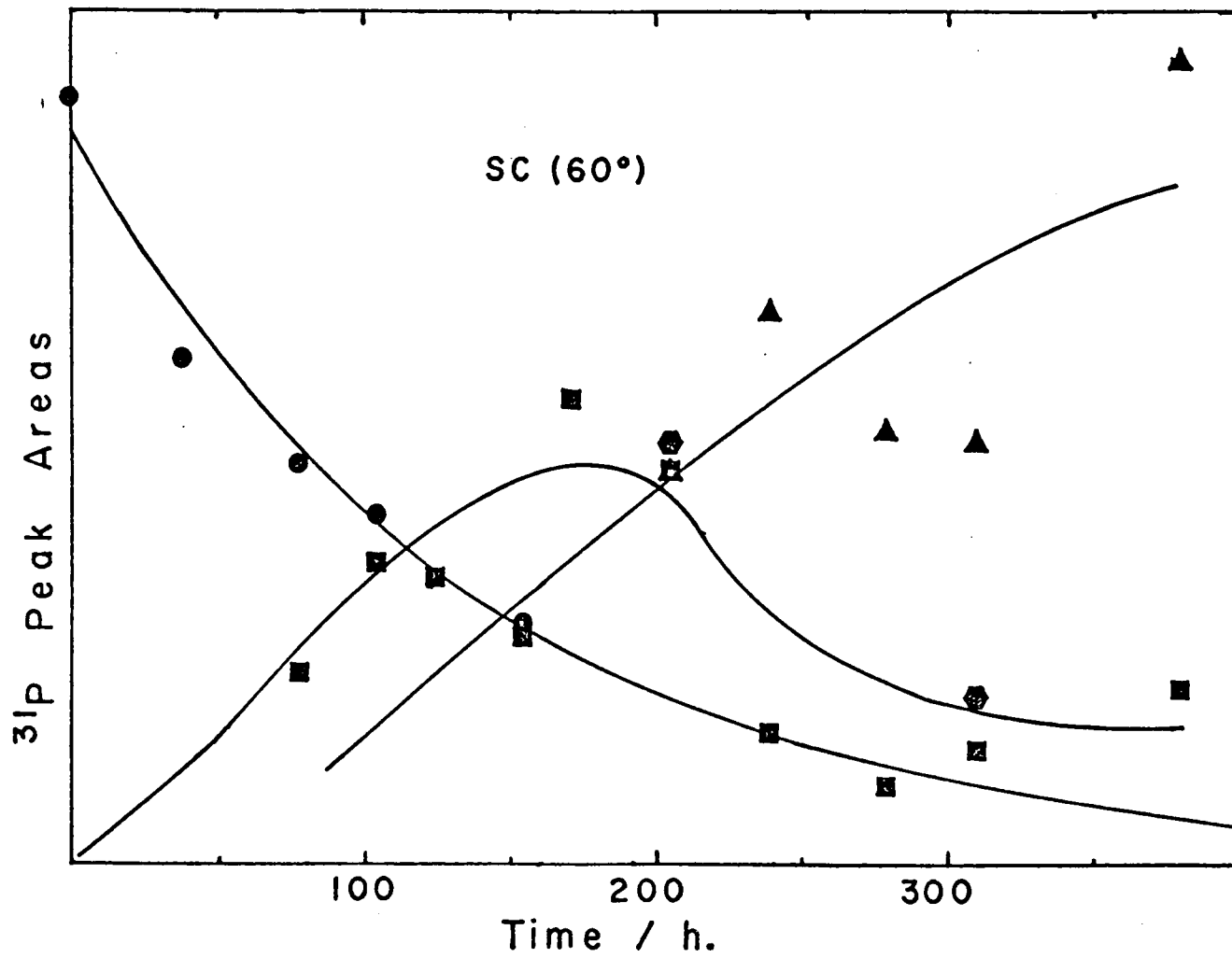


FIGURE 10

Time dependence of the ^{31}P peak areas during the degradation of supracide (circles) at +95.20 ppm to products at +65.2 ppm (squares), +34.2 ppm (hexagons), and +1.85 ppm (triangles). Temperature was 90°C; initial pH was 4.7.

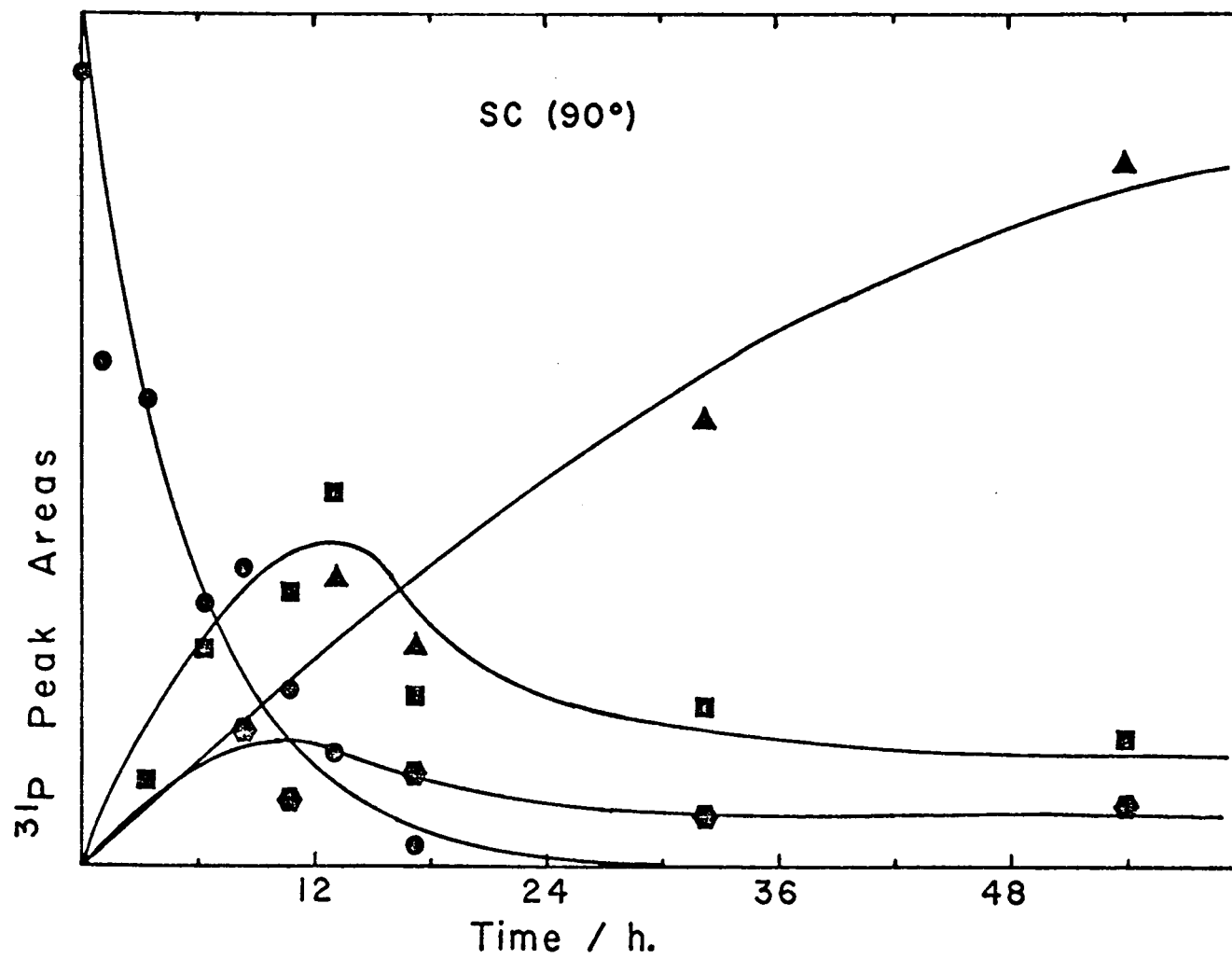


Table 9. Relative ^{31}P Peak Areas of Supracide and Its Degradation Products at 60°C.^g

Time/h	+95.20 ppm ^a	+65.2 ppm ^b	+34.2 ppm ^c	+1.85 ppm ^d	+100.0 ppm ^e	+61.8 ppm ^f
0.00	1.907					
38.12	1.266					
78.08	1.004	0.483				
104.64	0.878	0.749				
124.60	0.730	0.715				
154.41	0.467	0.566				
170.92		1.152				
205.23		0.983	1.052	0.983		
239.28		0.332		1.368		
278.89		0.195		1.075		
309.95		0.287	0.419	1.049		
379.46		0.444		1.982		
2031.22				2.861		

^a Supracide, $\text{SP}(\text{OMe})_2\text{SCH}_2\overline{\text{NC}(\text{O})\text{SC}(\text{OMe})\text{N}}$.

^b $\text{SP}(\text{OMe})_2(\text{OH})$.

^c Probably $\text{OP}(\text{OMe})(\text{OH})(\text{SMe})$.

^d Phosphates.

^e Probably $\text{SP}(\text{OMe})_2(\text{SMe})$.

^f Probably $\text{SP}(\text{OMe})(\text{OH})^-$.

^g In some spectra, a weak signal was visible at +24.9 ppm, possibly due to a phosphorothiolate.

Table 10. Relative ^{31}P Peak Areas of Supracide and Its Degradation Products at 70°C.^g

Time/h	+95.20 ppm ^a	+65.2 ppm ^b	+34.2 ppm ^c	+1.85 ppm ^d	+100.0 ppm ^e	+61.8 ppm ^f
0.00	2.552					
7.50	2.333					
21.05	2.144	1.235				
41.82	1.165	2.242	0.670	0.472		
52.37	0.462	1.363	0.538	1.418		
67.79	0.190	1.400	0.755	1.680	0.182	
86.16		1.635	0.984	2.405	0.492	
138.55		0.899	0.419	2.187	0.231	
181.31		0.485	0.642	2.921	0.469	
218.55		0.564	0.224	3.086		
1828.75				4.734		

^a Supracide, $\text{SP}(\text{OMe})_2\text{SCH}_2\text{NC}(\text{O})\text{SC}(\text{OMe})\text{N}$.

^b $\text{SP}(\text{OMe})_2(\text{OH})$.

^c Probably $\text{OP}(\text{OMe})(\text{OH})(\text{SMe})$.

^d Phosphates.

^e Probably $\text{SP}(\text{OMe})_2(\text{SMe})$.

^f Probably $\text{SPO}(\text{OMe})(\text{OH})^-$.

^g In some spectra, a weak signal was visible at +24.9 ppm, possibly due to a phosphorothiolate.

Table 11. Relative ^{31}P Peak Areas of Supracide and Its Degradation Products at 90°C .^g

Time/h	+95.20 ppm ^a	+65.2 ppm ^b	+34.2 ppm ^c	+1.85 ppm ^d	+100.0 ppm ^e	+61.8 ppm ^f
0.00	3.254					
1.08	2.065					
3.39	1.915	0.344				0.654
6.37	1.072	0.884				0.327
8.36	1.219	1.195	0.554			0.554
10.70	0.723	1.120	0.265			0.187
13.08	0.462	1.537		1.170	0.537	0.870
17.21	0.079	0.693	0.369	0.892		
32.27		0.657	0.190	1.828		
53.91		0.519	0.240	2.883		
79.79				2.356		
108.44				2.714		
181.45		0.365		2.321		

^a Supracide, $\text{SP}(\text{OMe})_2\text{SCH}_2\text{NC}(\text{O})\text{SC}(\text{OMe})\text{N}$.

^b $\text{SP}(\text{OMe})_2(\text{OH})$.

^c Probably $\text{OP}(\text{OMe})(\text{OH})(\text{SMe})$.

^d Phosphates.

^e Probably $\text{SP}(\text{OMe})_2(\text{SMe})$.

^f Probably $\text{SP}(\text{OMe})(\text{OH})^-$.

^g In some spectra, a weak signal was visible at +24.9 ppm, possibly due to a phosphorothiolate.

where k is the rate constant in units of reciprocal time, and the brackets denote concentration. From this equation, the half-life $t_{1/2}$ is found to be

$$t_{1/2} = -0.693/k \quad (4)$$

A plot of $\ln[\text{pesticide}]$ versus time should be linear with a slope of $-k$ if the reaction is indeed first order with respect to the pesticide. Within the often sizeable experimental error limits, this appeared to be true for all three compounds. Because of errors inherent in analyses using a linear fit after logarithmic transformation of Eq. (3), a nonlinear least-squares fit to the data in its exponential form was used (43). Rate constants and half-lives so determined are listed in Table 12. The values are estimated to be accurate within $\pm 15\%$. At all temperatures studied, ethyl parathion degrades slower than does methyl parathion and significantly slower than does supracide. This is reasonable, in view of the susceptibility of the P-S bond to hydrolysis, and of the tendency of methyl esters to undergo dealkylation much more readily than ethyl esters (1).

From the kinetic data in Table 12, information about the thermodynamics of the reactions can be obtained through use of the Arrhenius equation

$$k = A \exp(-E_a/RT) \quad (5)$$

A plot of $\ln k$ versus the reciprocal absolute temperature is shown in Figure 11, for the free pesticides. Table 13 lists the activation energies and pre-exponential factors obtained from the

Table 12. Rate Constants and Half-Lives of the Pesticides as a Function of Temperature.

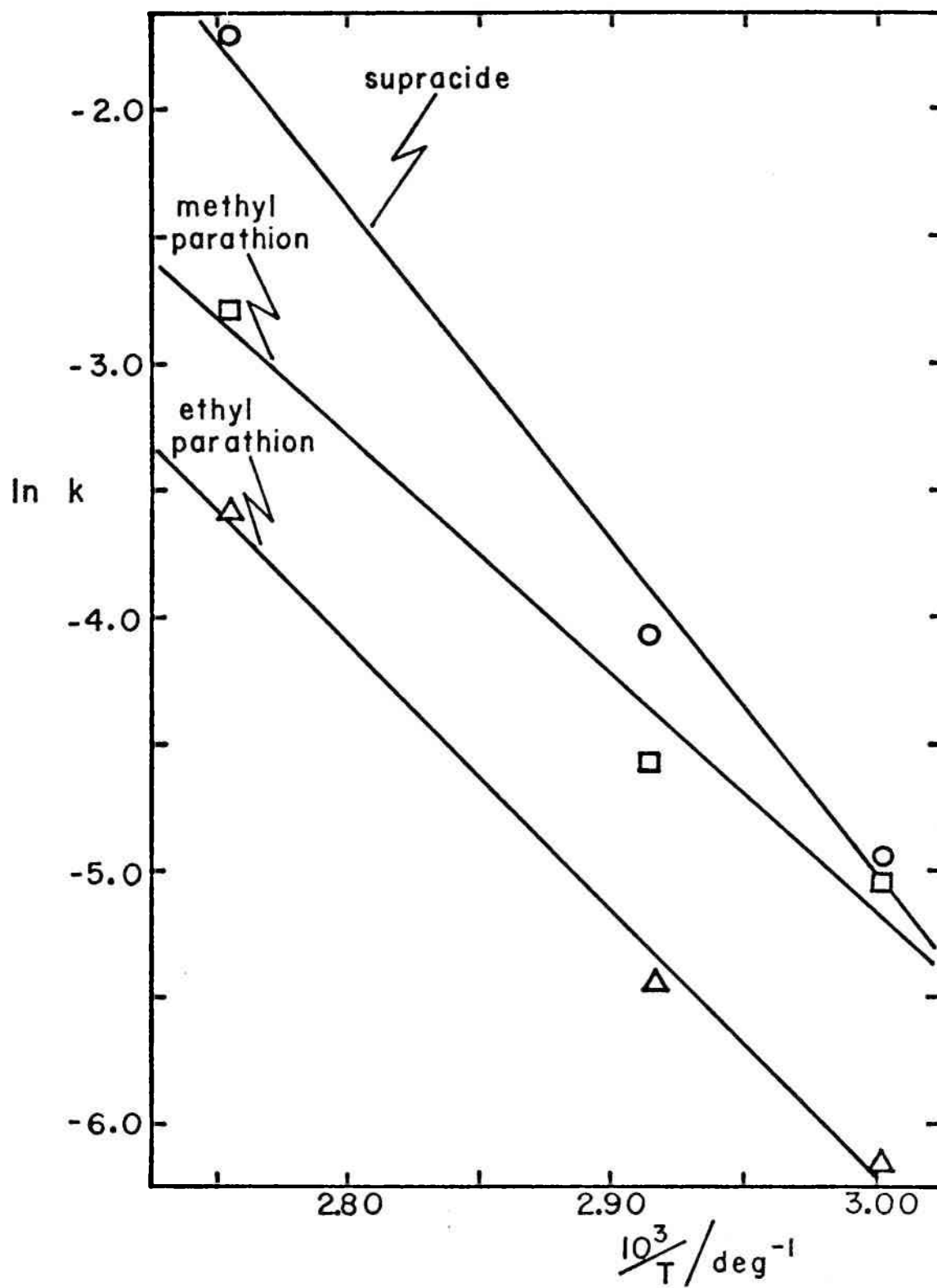
<u>Pesticide</u>	<u>Temperature/°C</u>	<u>k/h⁻¹</u>	<u>t^{1/2}/d</u>
Ethyl Parathion	60	2.1 x 10 ⁻³	13.7
	70	4.3 x 10 ⁻³	6.7
	90	2.5 x 10 ⁻²	1.2
Methyl Parathion	60	6.4 x 10 ⁻³	4.5
	70	1.0 x 10 ⁻²	2.8
	90	5.5 x 10 ⁻²	0.53
Supracide	60	7.1 x 10 ⁻³	4.0
	70	1.7 x 10 ⁻²	1.7
	90	1.8 x 10 ⁻¹	0.16

Table 13. Thermodynamic Data from Arrhenius Plots of Kinetic Data.

<u>Pesticide</u>	<u>A/h⁻¹</u>	<u>E_a/kcal mole⁻¹</u>
Ethyl Parathion	3 x 10 ¹⁰	20.1
Methyl Parathion	3 x 10 ⁹	17.7
Supracide	1 x 10 ¹⁵	26.3

FIGURE 11

Arrhenius plot for degradation of ethyl parathion (triangles), methyl parathion (squares), and supracide (circles).



Arrhenius plots. The values of E_a are certain within ± 1.5 kcal mole⁻¹; the values of A are reliable only to the nearest order of magnitude. It is known that the reactivity of organophosphorus compounds by hydrolysis decreases in the order phosphorothiolates>phosphates>phosphorothionates, and that activation energies for the first two types of compounds are 11.4 kcal mole⁻¹ and 14.9 kcal mole⁻¹, respectively (1). The 18-20 kcal mole⁻¹ values found for the phosphorothionate parathion pesticides are quite reasonable when compared with the numbers for the other two compound types in the series.

The kinetic analyses, as has been previously mentioned, were made using the simplifying assumption of pseudo-first-order kinetics; however, it is possible that consecutive, concurrent, and/or back reactions are occurring in some instances. Some of the fluctuation in peak areas reported in Tables 3-11 is due to errors caused in determining the area of the $P(OH)_4^+$ reference peak when it overlapped phosphate signals. The relative peak areas cannot be used for comparing concentrations of the different species, as no T_1 measurements were made to determine if differential saturation was occurring. There is evidence that ^{31}P T_1 's are dependent on solvent, pH, concentration, and ions in solution, among other factors (37). The effect of various relaxation reagents on the ^{31}P spin-lattice relaxation times of several kinds of phosphorus compounds has recently been published; the results are summarized in Table 14.

D. Future Research

One extremely simple improvement in experimental procedure for future studies would be the choice of another peak area and chemical shift reference to replace $P(OH)_4^+$, which is sometimes interfered with by phosphate resonances. A logical compound would appear to be P_4O_6 (38); its chemical shift of +112.5 ppm places it well out of the chemical shift ranges of nearly all of the compounds anticipated to occur in these studies (see Table 2).

Table 14. Effective Relaxation Reagents for ^{31}P NMR Observation of Organophosphorus Compounds.^{a,d}

<u>Compound Type</u>	<u>Structure</u>	<u>Relaxation Reagent</u>
alkyl phosphates	$(RO)_3P=O$	$\left. \begin{array}{l} \text{Fe(III)ethylene glycol} \\ \text{Fe(III)acac} \\ \text{Ni(II)} \\ \text{Cu(II)} \end{array} \right\}^b$
alkyl phosphonates	$(RO)_2(R)P=O$	
aryl phosphorothionates	$(PhO)_3P=S$	
alkyl phosphorothionates	$(RO)_3P=S$	
alkyl phosphorodithionates	$(RO)_2(RS)P=S$	$\left. \begin{array}{l} \\ \\ \end{array} \right\} \text{Gd(fod)}_3^c$
aryl phosphates	$(PhO)_3P=O$	

^a T_1 's decreased from 9-21 s to less than 1 s.

^b 1:1 relaxation reagent: organophosphorus compound. Cu(II) caused some broadening of resonances at these concentrations.

^c 100:1 relaxation reagent: organophosphorus compound.

^d From reference 32.

It is imperative that the dependence of T_1 on type and amount of relaxation reagent be quantitatively determined for the different compounds observed, to extend preliminary work in this area (32). Optimal types and concentrations of such reagents, and optimal pulse angles and pulse repetition times, can then be chosen to minimize or eliminate saturation effects, and to obtain correction factors, as necessary, for calculation of concentrations (44).

Positive assignment of peaks would be facilitated by studies of the pH dependence of the chemical shifts of a number of known compounds in their various neutral and anionic forms.

Lastly, the remainder of the pesticides in stock should be studied. Use of 10 mm, rather than 5 mm, tubes would greatly increase signal-to-noise and the attainable accuracy.

E. References

1. M. Eto, "Organophosphorus Pesticides: Organic and Biological Chemistry", CRC Press, Cleveland, Ohio, 1974.
2. R.D. O'Brien, "Insecticides: Action and Metabolism", Academic Press, New York, 1967.
3. "Fate of Pesticides in Environment" (A.S. Tahori, ed.), Gordon and Breach, New York, 1972.
4. C. Fest and K.-J. Schmidt, "The Chemistry of Organophosphorus Pesticides: Reactivity, Synthesis, Mode of Action, Toxicology", Springer-Verlag, New York, 1973.
5. N.N. Melnikov, "Chemistry of Pesticides", Springer-Verlag, New York, 1971.
6. B.C. Saunders, "Some Aspects of the Chemistry and Toxic Action of Organic Compounds Containing Phosphorus and Fluorine", Cambridge University Press, London, 1957.
7. H.G. Kohrana, "Some Recent Developments in the Chemistry of Phosphate Esters of Biological Interest", John Wiley and Sons, New York, 1961.
8. D.F. Heath, "Organophosphorus Poisons, Anticholinesterases, and Related Compounds", Pergamon Press, Oxford, 1961.
9. R.D. O'Brien, "Toxic Phosphorus Esters: Chemistry, Metabolism, and Biological Effects", Academic Press, New York, 1960.
10. R.L. Metcalf, "Organic Insecticides - Their Chemistry and Mode of Action", Interscience, New York, 1955.
11. G.M. Kosolapoff, "Organophosphorus Compounds", John Wiley and Sons, New York, 1950.
12. A.J. Kirby and S.G. Warren, "The Organic Chemistry of Phosphorus", Elsevier, Amsterdam, 1967.
13. R.F. Hudson, "Structure and Mechanism in Organophosphorus Chemistry", Academic Press, London, 1965.
14. "Phosphorus and its Compounds" (J.R. van Wazer, ed.), Vol. I (1958) and Vol. II (1961), Interscience, New York.
15. L.H. Keith and A.L. Alford, J. Ass. Offic. Anal. Chem., 53, 1018 (1970).
16. L.H. Keith, A.W. Garrison, and A.L. Alford, J. Ass. Offic. Anal. Chem., 51, 1063 (1968).

17. L.H. Keith and A.L. Alford, "Catalog of Pesticide NMR Spectra", Water Pollution Control Research Series #16020 EWC, Environmental Protection Agency, Raleigh, North Carolina, 1971.
18. A.W. Garrison, L.H. Keith, and A.L. Alford, "Fate of Organic Pesticides in the Aquatic Environment", American Chemical Society, Washington, DC, 1972.
19. L.H. Keith and A. Alford, Anal. Chim. Acta, 44, 447 (1969).
20. Z.L.F. Gaibel and L. Fishbein, Va. J. Sci., 21, 14 (1970).
21. N.F. Janes, A.F. Machin, M.P. Quick, H. Rogers, D.E. Mundy, and A.J. Cross, J. Agr. Food Chem., 21, 121 (1973).
22. T.M. Ward, I.L. Allcox, and G.H. Wahl, Jr., Tetrahedron Letters, 4421 (1971).
23. H. Babad and W. Herbert, Anal. Chim. Acta, 41, 259 (1968).
24. R. Haque, W.R. Coshaw, and L.F. Johnson, J. Amer. Chem. Soc., 91, 3822 (1969).
25. B.E. Pape and M.J. Zabik, J. Agr. Food Chem., 18, 202 (1970).
26. J.A. Durden, H.W. Stollings, J.E. Casida, and M. Slade, J. Agr. Food Chem., 18, 459 (1970).
27. R. Haque and D.R. Buhler, Ann. Rep. NMR Spectroscopy, 4, 237 (1971).
28. "Environmental Science Research, Vol. 4: Mass Spectrometry and NMR Spectroscopy in Pesticide Chemistry" (R. Haque and F.J. Biros, eds.), Plenum Press, New York, 1974.
29. N. Muller and J. Goldensen, J. Amer. Chem. Soc., 78, 5182 (1956).
30. T.R. Fukuto, E.O. Hornig, and R. Metcalf, J. Agr. Food Chem., 12, 169 (1964).
31. R.T. Ross and F.J. Biros, Anal. Chim. Acta, 52, 139 (1970).
32. T.W. Gurley and W.M. Ritchey, Anal. Chem., 48, 1137 (1976).
33. A.E. Lippman, J. Org. Chem., 30, 3217 (1965).
34. R.A.Y. Jones and A.R. Katritzky, Angew. Chem., 74, 60 (1962).
35. D.W. Allen, B.G. Hutley, and M.T.J. Mellor, J.C.S. Perkin II, 789 (1977).

36. A.J.R. Costello, T. Glonek, and J.R. van Wazer, Inorg. Chem., 15, 972 (1976).
37. T. Glonek, J. Amer. Chem. Soc., 98, 7090 (1976).
38. "Topics in Phosphorus Chemistry, Vol. 5: ^{31}P Nuclear Magnetic Resonance" (M. Grayson and E.J. Griffith, eds.), Interscience, New York, 1967.
39. T. Glonek and J.R. van Wazer, J. Magn. Resonance, 13, 390 (1974).
40. W.M. Latimer, "The Oxidation States of the Elements and Their Potentials in Aqueous Solutions", Prentice-Hall, Englewood Cliffs, New Jersey (1952).
41. E.M. Hyde, J.D. Kennedy, B.L. Shaw, and W. McFarlane, J.C.S. Dalton, 1571 (1977).
42. D.J. Pietrzyk and C.W. Frank, "Analytical Chemistry: An Introduction", Academic Press, New York, 1974, p. 651.
43. G.H. Schmid, V.M. Csizmadia, P.G. Mezey, and I.G. Csizmadia, Can. J. Chem., 54, 3330 (1976).
44. K.A. Christiansen, D.M. Grant, E.M. Schulman, and C. Walling, J. Phys. Chem., 78, 1971 (1974).

APPENDIX

A Paper Entitled

"The T_1 of the $^{205}\text{Tl}^+$ Ion in DMSO: A Case
of the Importance of Chemical
Shift Anisotropy"

The T_1 of the $^{205}\text{Tl}^+$ Ion in DMSO: A Case
of the Importance of Chemical
Shift Anisotropy

by

J. F. Hinton
Department of Chemistry
University of Arkansas
Fayetteville, Arkansas 72701

K. H. Ladner
Department of Chemistry
University of Western New Mexico
Silver City, New Mexico 88061

The spin-lattice relaxation properties of metal ions have been the subject of a number of recent studies. For example, the spin-lattice relaxation times, T_1 , of ions such as $^{207}\text{Pb}^{+2}$ (1,2), $^{113}\text{Cd}^{+2}$ (3), $^{133}\text{Cs}^{+}$ (4-6), $^{85}\text{Rb}^{+}$ (5), $^{87}\text{Rb}^{+}$ (5,6), $^{23}\text{Na}^{+}$ (5,6), $^9\text{Be}^{+2}$ (7), $^7\text{Li}^{+1}$ (5,6,8-11), $^6\text{Li}^{+1}$ (12), $^{199}\text{Hg}^{+2}$ (13), and $^{205}\text{Tl}^{+}$ (14,15) have been determined and the mechanisms responsible for the relaxation behavior explored. With few exceptions (e.g. 1), the contribution from chemical shift anisotropy (CSA) to the total relaxation time has not been experimentally investigated. We wish to present a case for the importance of CSA in determining the relaxation behavior of a metal ion. The T_1 of the $^{205}\text{Tl}^{+}$ (spin $I=1/2$) ion in DMSO has been found to have a significant dependence on transient anisotropic chemical shielding interactions.

The spin-lattice relaxation experiments were performed on a modified Bruker HFX-90 spectrometer interfaced to a Nicolet NIC 80 computer and operating in the pulsed-FT mode at a field strength of 2.114T with ^1H field lock. The spin-lattice relaxation times were obtained by using the inversion-recovery sequence with phase inversion on alternate pairs of observing pulses. The inversion-recovery data were analyzed using a non-linear least-squares computer program to obtain the spin-lattice relaxation times. The spin-lattice relaxation time values presented are the averages of at least two different measurements in all cases. The TlNO_3 and TlClO_4 salts used were recrystallized from high purity water at least twice. Canada Isotopes, Merck Chemical Div-

ision, DMSO-d₆ with a minimum isotope purity of 99.5 atom % deuterium was used without further purification. The non-deuteriated DMSO used was Fisher reagent grade that had been triply distilled. All solutions were prepared in a glove box in a dry atmosphere, carefully degassed in 5 mm NMR tubes using the freeze-thaw method (six or seven cycles) and then sealed. The probe temperature was maintained to ± 0.5 degrees.

In solution the spherical symmetry of a monatomic ion, such as Tl⁺, becomes distorted because of interactions with solvent molecules, counterions, and in very concentrated solutions, other cations. With increasing concentration, ion-ion interactions become important, manifesting themselves in the replacement of adjacent solvent molecules by counterions. The formation of transient ion-pairs produces an extremely large perturbation in the electronic environment of the nucleus of interest (i.e. ²⁰⁵Tl⁺). The effect of transient counterion penetration of the solvation sphere of an ion is the production of a fluctuating electronic distribution about the nucleus (i.e. ²⁰⁵Tl⁺). The transient formation of ion-pairs creates a modulation of the magnitude of the components and orientation of the principal axes of the chemical shielding tensor, as well as the reorientation of the solvated ion (Tl⁺), providing a mechanism for spin-lattice relaxation. This mechanism is called transient chemical shift anisotropy (16). The contribution to spin-

lattice relaxation from transient CSA is predicted to be quite large for the $^{205}\text{Tl}^+$ ion. Shielding anisotropies for covalently bonded ^{205}Tl are of the order of 1000-3000 ppm (16). Shielding anisotropies of ion-pairs are thought to be of the same order of magnitude (16).

Figure 1 shows a plot of the spin-lattice relaxation time of the $^{205}\text{Tl}^+$ ion in DMSO at 295K as a function of the concentration of TlNO_3 and TlClO_4 salts. These results illustrate the concentration and counterion dependence of the spin-lattice relaxation time of the $^{205}\text{Tl}^+$ ion in DMSO. The presence of transient CSA is obvious.

A qualitative assessment of the magnitude of the transient CSA mechanism contribution to the total spin-lattice relaxation time can be inferred from the temperature dependence of the T_1 . Figure 2 shows plots of $\ln T_1$ against the reciprocal of the absolute temperature for three concentrations of TlClO_4 . For the 0.15 M solution, transient spin-rotation is the dominant relaxation mechanism since the T_1 decreases with increasing temperature (17), assuming scalar coupling modulated by chemical exchange is not significant (2). The presence of contributions by other relaxation processes is evidenced by the non-linearity of this plot. Relaxation can arise from local fields produced by spin-rotation. A molecular system possessing angular velocity constitutes a rotating charge system and, therefore, a magnetic field is produced and experienced by the resonant nucleus. Modulation

of both the direction and magnitude of the angular momentum vector associated with the rotating molecule produces fluctuations in the magnetic field. Although the first solvation sphere of an ion is probably not composed of a well defined molecular species, if one assumes the existence of transient species capable of reorientating as a molecular unit over an interval of the order of 10^{-11} sec, then transient spin-rotation can significantly contribute to the total relaxation process. In general, when one is dealing with small symmetric molecular entities and with nuclei which have a large chemical shift range, such as ^{205}Tl , one can anticipate that spin-rotation will contribute significantly to the relaxation. The correlation between chemical shift and spin-rotation interaction arises because both the chemical shift and spin-rotation tensor components depend upon the electron distribution (17, 18).

As the concentration of TlClO_4 increases the transient CSA contribution becomes more significant. For the 0.99 M TlClO_4 solution at 22°C transient CSA and SR contributions are approximately equal. For the 2.99 M TlClO_4 solution at 22°C , the transient CSA relaxation mechanism becomes dominant.

The direction of the slope of the $\ln T_1$ vs. $1/T$ K plot at low temperatures for the 2.99 M TlClO_4 solution is indicative not only of the transient CSA relaxation mechanism but also of the dipolar and scalar-coupling of the second kind mechanisms. The dipolar relaxation would be assumed

to arise from interactions between the ^{205}Tl nucleus and the solvation DMSO protons or oxygen-17. The dipolar contribution from the protons of DMSO molecules, however, was determined to be insignificant since no change in spin-lattice relaxation time was observed when DMSO- d_6 was used as the solvent. A dipolar contribution from ^{17}O is assumed to also be negligible in this system as well as a scalar coupling contribution (1, 3).

Acknowledgment: We wish to acknowledge the support provided by the United States Department of the Interior, Office of Water Resources and Technology, as provided for under Public Law 88-379 through a grant A-030-Arkansas.

References

1. R. M. Hawk and R. R. Sharp, *J. Chem. Phys.*, 60, 1522 (1974).
2. R. M. Hawk and R. R. Sharp, *J. Magn. Resonance*, 10, 385 (1973).
3. M. Holz, R. B. Jordan and M. D. Zeidler, *J. Magn. Resonance*, 22, 47 (1976).
4. F. W. Wehrli, *J. Magn. Resonance*, 25, 575 (1977).
5. H. G. Hertz, M. Holz, G. Keller, H. Versmold and C. Yoon, *Ber. Bunsenges. Phys. Chem.*, 78, 493 (1974).
6. C. A. Melendres and H. G. Hertz, *J. Chem. Phys.*, 61, 4156 (1974).
7. F. W. Wehrli, *J. Magn. Resonance*, 23, 181 (1976).
8. A. I. Mishustin and Yu. M. Kessler, *J. Solution Chem.*, 4, 779 (1976).
9. D. E. Woessner, B. S. Snowden and A. G. Ostroff, *J. Chem. Phys.*, 49, 371 (1968).
10. H. G. Hertz, R. Tutsch and H. Versmold, *Ber. Busenges. Phys. Chem.*, 75, 1177 (1971).
11. G. S. Bystrov and N. I. Nikolaev, *Russ. J. Phys. Chem.*, 47, 522 (1973).
12. F. W. Wehrli, *J. Magn. Resonance*, 23, 527 (1976).
13. G. Maciel and M. Borzo, *J. Magn. Resonance*, 10, 388 (1973).
14. M. Bacon and L. Reeves, *J. Amer. Chem. Soc.*, 95, 272 (1973).
15. S. O. Chan and L. Reeves, *J. Amer. Chem. Soc.*, 96, 404 (1974).

16. R. N. Schwartz, *J. Magn. Resonance*, 24, 205 (1976).
17. T. C. Farrar and E. D. Becker, "Pulse and Fourier Transform NMR", Academic Press, New York, 1971.
18. C. Deverell, *Mol. Phys.*, 18, 319 (1970).
19. J. F. Hinton and R. W. Briggs, *J. Magn. Resonance*, 25, 379 (1977).

Figure 1. Plots of the T_1 of the $^{205}\text{Tl}^+$ ion as a function of concentration for the salts TlNO_3 and TlClO_4 at 22°C . The extrapolated value of 1.92 sec. is compared to the previously determined value of 1.8 sec. for a 0.2 M TlNO_3 -DMSO solution (19). The previously reported value was inadvertently listed as 0.18 sec.

Figure 2. Plots of $\ln T_1$ against the reciprocal of the absolute temperature for 0.15 M, 0.99 M and 2.99 M TlClO_4 solutions.

